Implementation and calibration of a stochastic multicloud convective parameterization in the NCEP Climate Forecast System (CFSv2)

B. B. Goswami[1], B Khouider[1], R Phani[2], P Mukhopadhyay[2], and A.J. Majda[3,4]

[1]Department of Mathematics and Statistics, University of Victoria, BC, Canada.
[2]Indian Institute of Tropical Meteorology, Pune, India
[3]Department of Mathematics and Center for Atmosphere and Ocean Sciences, Courant Institute for Mathematical Sciences, New York University, New York, USA
[4]Center for Prototype Climate Models, New York University-Abu Dhabi, Abu Dhabi, United Arab Emirates

Key Points:

- Stochastic convective parameterization via a multicloud model
- Evaluation of parameter regime for the stochastic parameterization
- Model tuning focusing on the mean state and the intra-seasonal variability

Corresponding author: B. B. Goswami, `bgoswami@uvic.ca`

Abstract

A comparative analysis of 14 5-year long climate simulations produced by the National Centres for Environmental Predictions (NCEP) Climate Forecast System version 2 (CFSv2), in which a stochastic multicloud (SMCM) cumulus parameterization is implemented, is presented here. These 5-year runs are made with different sets of parameters in order to figure out the best model configuration based on a suite of state-of-the-art metrics. This analysis is also a systematic attempt to understand the model sensitivity to the SMCM parameters. The model is found to be resilient to minor changes in the parameters used implying robustness of the SMCM formulation. The model is found to be most sensitive to the mid-tropospheric dryness parameter (MTD) and to the stratiform cloud decay timescale (τ_{30}). MTD is more effective in controlling the global mean precipitation and its distribution while τ_{30} has more effect on the organization of convection as noticed in the simulation of the Madden-Julian oscillation (MJO). This is consistent with the fact that, in the SMCM formulation, mid-tropospheric humidity controls the deepening of convection and stratiform clouds control the backward tilt of tropospheric heating and the strength of unsaturated downdrafts which cool and dry the boundary layer and trigger the propagation of organized convection. Many other studies have also found mid-tropospheric humidity to be a key factor in the capacity of a global climate model to simulate organized convection on the synoptic and intra-seasonal scales.

1 Introduction

The successful implementation of any convective parameterization scheme, any parameterization scheme for that matter, involves formulation, assessment and tuning. Formulation is the process of designing and implementing the model equations from first principles. Once the scheme is formulated, assessment and tuning evolve simultaneously. Due to the complex nature of the climate system and the inherent uncertain parameters of the scheme, tuning is unavoidable and it is time consuming. *Hourdin et al.* [2016] views tuning as a work of “art”, than a mere engineering calibration exercise, as it involves skill gained through observation and experience. In their survey, they found that 96% of climate models evolve through the process of tuning. They also found that cumulus schemes to be the most commonly tuned parameterizations in a climate model, second to microphysics schemes.

Convective parameterizations are traditionally deterministic [*Palmer*, 2001; *Plant and Craig*, 2008]. The basis for a deterministic convective parameterization is the underlying assumption that, a typical GCM grid size is large enough to contain a large ensemble of the clouds, which is in quasi-equilibrium with the large scales [*Arakawa and Schubert*, 1974]. However, with the increasing resolution of the present day GCMs, the validity of this assumption needs to be reevaluated [*Palmer*, 1996]. Moreover, there is an undeniable possibility that neglecting the variability of the subgrid scale convective elements may lead to biases in the mean climate [*Palmer*, 2001]. Many recent studies have showed that a stochastic approach to the convective parameterization problem can be promising [*Buizza et al.*, 1999; *Lin and Neelin*, 2000, 2002, 2003; *Palmer*, 2001; *Majda and Khouider*, 2002; *Khouider et al.*, 2003; *Plant and Craig*, 2008; *Teixeira and Reynolds*, 2008; *Deng et al.*, 2015, 2016; *Ajayamohan et al.*, 2016; *Davini et al.*, 2016]. In order to introduce stochasticity to an existing deterministic convective parameterization (CP), different methods have been adopted. The perturbed parameterization tendencies approach introduced by *Buizza et al.* [1999] consists of multiplying the CP outputs by correlated or non-correlated random numbers at each GCM column [*Davini et al.*, 2016, and references therein]. *Teixeira and Reynolds* [2008] followed a similar technique as *Buizza et al.* [1999] but they multiplied only the convective tendencies. *Lin and Neelin* [2000] had added stochasticity to a deterministic scheme by adding zero-mean red noise to it. In the study by *Lin and Neelin* [2002], a distribution of precipitation is assumed a priori to control the statistics of the overall convective heating. *Lin and Neelin* [2003] tested a stochastic deep convective parameterization in a general circulation model for the first time. *Plant and Craig* [2008] used equilibrium statistical mechanics to derive a Poisson distribution for convective plumes based on radiative convective equilibrium cloud resolving simulations. *Majda and Khouider* [2002] and *Khouider et al.* [2003] used a Markov process on a lattice for convective inhibition. The stochastic lattice approach has been extended in *Khouider et al.* [2010] to derive the stochastic multicloud model (SMCM). The SMCM has been extensively used and evaluated in simple models for organized convection and convectively coupled equatorial waves (CCEW) [*Frenkel et al.*, 2012, 2013; *Peters et al.*, 2013; *De La Chevrotière et al.*, 2015; *De La Chevrotière and Khouider*, 2017]. The SMCM has been successfully adopted as a cumulus parameterization in an aquaplanet GCM to simulate the Madden-Julian oscillation (MJO), CCEWs and Indian summer monsoon intra-seasonal oscillations (MISOs) [*Deng et al.*, 2015, 2016; *Ajayamohan et al.*, 2016]. This study investigates the impact of the stochastic multicloud model when implemented in a comprehensive climate model, namely, the National Centres for Environmental Predictions (NCEP) Climate Forecast System version 2 (CFSv2) model [*Saha et al.*, 2014]. Noteworthy, here we do not add stochasticity to the existing CP scheme in CFSv2. Rather, we completely replace it with the stochastic multicloud model. For brevity, the coupled CFSv2_SMCM model is termed as CFSsmcm. The first results of the implementation of the SMCM in CFSv2 have appeared in *Goswami et al.* [2017a], followed by a thorough analysis of the results in *Goswami et al.* [2017b]. CFSsmcm is found not only to improve some of the known biases of CFSv2 associated with organized tropical convection but it also captures the main physical and dynamical features of the major modes of tropical variability such as the MJO, CCEWs and the MISO [*Goswami et al.*, 2017b]. *Peters et al.* [2017] used the SMCM to control the triggering of deep convection and correct deficiencies in the ECHAM model, resulting in important improvements in its ability to simulate climate variability associated with organized convection, including the MJO and CCEWs. The SMCM framework has been also used by *Dorrestijn et al.* [2013a,b, 2015, 2016] with one key difference of using large eddy simulation data to infer the transition probabilities, a discrete-time Markov chain, conditional on the large scale predictors, instead of using Arrhenius-type activation functions to define transition rates, of a continuous time Markov process, as functions of the large scale predictors as done originally [*Khouider et al.*, 2010].

Notably the implementation of the SMCM in the CFSv2 model, assessed and calibrated here, is done essentially in order to improve the simulation of convective organization and variability, especially in the tropics. In its conventional form, CFSv2 uses the Simplified Arakawa-Schubert (SAS) [*Pan and Wu*, 1995; *Pattanaik et al.*, 2013] scheme for convection parameterization. SMCM was introduced in *Khouider et al.* [2010] following the inception of the multi-cloud model approach in its deterministic form [*Khouider and Majda*, 2006]. It is designed to capture the organization and variability of tropical convection by promoting the three cloud types that are observed to dominate organized tropical convective systems [*Lin and Johnson*, 1996; *Johnson et al.*, 1999; *Mapes et al.*, 2006; *Moncrieff et al.*, 2012], namely, congestus, deep and stratiform. The cloud coverage, associated with each cloud type, within a GCM grid, evolves as a stochastic Markov process with transition probabilities depending on the large scale mid-tropospheric dryness (MTD), convective available potential energy (CAPE), convective inhibition (CIN) and the large scale vertical velocity (W) [*Goswami et al.*, 2017a]. These large scale variables are normalized by some reference values and the normalized values are used in a birth-death Markov chain process for the different clouds to grow, decay and transition from one type to another. The choice of the reference values of the convective available potential energy (CAPE) and the mid-tropospheric dryness (MTD) are shown to be crucial for the dynamics of the stochastic cloud fractions [*Khouider et al.*, 2010]. The simulation of the MJO and CCEWs are found to be sensitive to the longevity of stratiform heating [*Ajayamohan et al.*, 2016; *Deng et al.*, 2016]. In fact, all the earlier studies involving SMCM [e.g. *Khouider et al.*, 2010; *Deng et al.*, 2015; *Ajayamohan et al.*, 2016; *Deng et al.*, 2016] agree that the parameters responsible for the magnitude of the stratiform heating, and the transition time scales between different cloud types are among the most uncertain parameters. *De La Chevrotière et al.* [2015] have used a Baysian inference procedure to learn the cloud transition time scales from large eddy simulation data (GigaLES) from the Global Atmospheric Research Programme (GARP) Atlantic Tropical

Experiment (GATE) field campaign [*Khairoutdinov et al.*, 2009]. While De La Chevrotiere et al's study provides reference values for these parameters their precise values remain uncertain as the tropical Atlantic region is not per se representative of the whole tropical atmosphere which is characterized by various meteorological regimes that depend strongly on the geography.

Moreover, while the earlier studies involving the SMCM provide some directions for tuning the CFSsmcm, several aspects are totally new to the present implementation. The differences are obvious as the previous studies were carried out in an aquaplanet idealized framework and they all rely on the radiative convective equilibrium (RCE) solution of the governing equations to construct the background to set up the multi-cloud parameterization. Instead, in the present study, we use the long term mean of the observed climate as the background. Also, unlike the aqua-planet framework, used in the previous studies, here, we use CFSv2 as the host model, which is a fully coupled state-of-the-art climate model. This is the first time the SMCM has been implemented in a coupled climate model. It is motivated by the success of the SMCM in the aqua-planet setup. Due to the significant modifications in the SMCM formulation done in order to make it compatible with the CFSv2, the CFSsmcm model requires tuning. As a prerequisite to simulate a realistic climate, it is necessary to understand, how CFSv2 responds to the implementation of the SMCM in it. Does the SMCM retain its major behavioral features seen in the idealized setup? How sensitive is the SMCM to the new set of parameters introduced in the present formulation, especially, regarding the parameters associated with the background? Consequently, the aim of this study is to figure out the best suite of parameters for the CFSsmcm model. With the primary interest behind implementing the SMCM in CFSv2 being to improve the simulation of organization and variability of tropical convection, we have essentially made 5-year long climate runs for different sets of parameters. These runs are tuned for the mean climate, defined in terms of temperature, moisture and precipitation and then fine-tuned for the capability to capture the intraseasonal and synoptic variability associated with convectively coupled waves as measured by the Takayabu-Wheeler-Kiladis spectra [*Takayabu*, 1994; *Wheeler and Kiladis*, 1999].

The paper is organized as follows. A brief description of the SMCM model formulation is presented in Section 2 to introduce the tunable parameters involved. Section 3 describes the sensitivity of the model to different parameters. Finally, a few concluding remarks are provided in Section 4.

2 Model Equations, Data, and Methodology

The stochastic multicloud model (SMCM) uses 3 prescribed profiles for convective heating, ϕ_c, ϕ_d and ϕ_s, associated with cumulus congestus cloud decks (which warm and moisten the lower troposphere and cool the upper troposphere through radiation and detrainment), deep cumulus clouds (which heat up the whole atmospheric column) and stratiform anvils (which heat the upper troposphere and cool and moisten the lower troposphere through melting and evaporation of stratiform precipitation), respectively [*Khouider and Majda*, 2006, 2008; *Khouider et al.*, 2011]

The total convective heating is thus expressed as:

$$Q_{tot}(z) = H_d \phi_d(z) + H_c \phi_c(z) + H_s \phi_s(z). \tag{1}$$

Here, H_c, H_d and H_s are the parameterized heating rates associated with the three cloud types, congestus, deep, and stratiform, respectively. In particular, they are assumed to be proportional to the stochastically evolving area fractions, σ_c, σ_d and σ_s, respectively. We

Table 1. SMCM transition rules. The transition rates are given in terms of the large scale predictors CAPE, $C = CAPE/CAPE0$, Low level CAPE, $C_L = LCAPE/LCAPE0$, dryness, $D = \mathcal{H}/MTD0$, where $\mathcal{H}$ is the relative humidity, large scale subsidence, $W_N = -\min(0, W/W0)$, and $C_N = -CIN/CIN0$. Here $LCAPE$ is the part of the CAPE integral between LFC and the freezing level. We note that CIN is by definition a negative definite quantity, so that when CIN is large, $\Gamma(C_N) \longrightarrow 1$.

Description	Transition Rate, where $\Gamma(x) = \begin{cases}(1-e^{-x}), & \text{if } x > 0\\ 0, & \text{otherwise}\end{cases}$	Time Scale (hours)
Formation of congestus	$R_{01} = \frac{1}{\tau_{01}}\Gamma(C_L)\Gamma(D)\frac{\mathbf{(1-\Gamma(W_N))+(1-\Gamma(C_N))}}{\mathbf{2}}$	τ_{01}=32
Decay of congestus	$R_{10} = \frac{1}{\tau_{10}}\Gamma(D)$	τ_{10}=2
Conversion of congestus to deep	$R_{12} = \frac{1}{\tau_{12}}\Gamma(C)(1-\Gamma(D))$	τ_{12}=0.25
Formation of deep	$R_{02} = \frac{1}{\tau_{02}}(\Gamma(C)(1-\Gamma(D))\frac{\mathbf{(1-\Gamma(W_N))+(1-\Gamma(C_N))}}{\mathbf{2}}$	τ_{02}=12
Conversion of deep to stratiform	$R_{23} = \frac{1}{\tau_{23}}$	τ_{23}=0.25
Decay of deep	$R_{20} = \frac{1}{\tau_{20}}(1-\Gamma(C))$	τ_{20}=9.5
Decay of stratiform	$R_{30} = \frac{1}{\tau_{30}}$	τ_{30}=1

have:

$$H_d = \frac{\sigma_d}{\bar{\sigma_d}} Q_d \tag{2}$$

$$H_c = \frac{\sigma_c}{\bar{\sigma_c}} \alpha_c Q_c \tag{3}$$

$$\frac{\partial H_s}{\partial t} = \frac{1}{\tau_s}\left[\frac{\sigma_s}{\bar{\sigma_s}}\alpha_s H_d - H_s\right], \tag{4}$$

here, $\bar{\sigma_c}$, $\bar{\sigma_d}$ and $\bar{\sigma_s}$ are the background values of σ_c, σ_d and σ_s respectively while α_c and α_s are respectively the congestus and stratiform adjustment coefficients and τ_s is the stratiform heating adjustment time-scale [*Khouider et al.*, 2010; *Deng et al.*, 2015].

The cloud area fractions σ_c, σ_d and σ_s are derived through the coarse graining of a stochastic lattice model taking the values 0,1,2, or 3, at each lattice site, according to whether the site is not cloudy (abusively called clear sky although it may support shallow convection) or occupied by a congestus, deep, or stratiform cloud type. Together they describe a Markov jump stochastic process in the form of a multi-dimensional birth-death system whose transition probabilities depend explicitly on some key large scale predictors motivated by observations and physical intuition [*Khouider et al.*, 2010; *Frenkel et al.*, 2012; *Peters et al.*, 2013; *Deng et al.*, 2016]. The interested reader is referred to these original papers for details. While earlier versions of the SMCM use only mid tropospheric dryness (MTD) and convective available potential energy (CAPE) as large scale predictors, here we also use convective inhibition (CIN) and vertical velocity (W) in order to obtain a better dialog between the deep convection parameterization, i.e., SMCM, and CFSv2's shallow convection scheme, by inhibiting congestus and deep convective clouds in regions of high CIN and/or large-scale subsidence. Therefore the transition rates from one cloud type to another remain the same as prescribed in *Deng et al.* [2015], for example, except for the formation of congestus and deep convection from clear sky. The transition rates closure equations are provided in Table 1 where the new modifications are highlighted in bold.

In Eqn (2-4), Q_c and Q_d are the potentials for congestus and deep convection which are closed following the equations [*Khouider et al.*, 2010; *Deng et al.*, 2015],

$$Q_d = \left[\bar{Q_d} + \frac{1}{\tau_q}\frac{L_v}{C_p}q_m^{'} + \frac{1}{\tau_c}\left(\theta_{eb}^{'} - \gamma_c\theta_m^{'}\right)\right]^+ \tag{5}$$

$$Q_c = \left[\bar{Q_c} + \frac{1}{\tau_c}\left(\theta_{eb}^{'} - \gamma_c\theta_m^{'}\right)\right]^+ \tag{6}$$

Here and elsewhere in the paper X^+ and X^- denote, respectively, the positive and negative parts of the variable $X\ :\ X^+ = max(X,0)$ and $X^- = min(X,0)$. The variables θ, θ_e and q denote potential temperature, equivalent potential temperature and moisture (specific humidity). L_v is the latent heat of condensation and C_p is the specific heat of air at constant pressure. The bar-ed notations indicate fixed background values and the prime-ed notations indicate deviations of the large scale GCM variables from the background variables. The suffix m stands for the middle troposphere value and b for the bulk boundary layer value, namely,

$$\begin{aligned} \theta_m &= \theta(500hPa) \\ q_m &= q(700hPa) \\ X_b &= \frac{1}{h}\int_0^h X(z)dz, \text{where } h \text{ is the GCM PBL height} \end{aligned}$$

In addition to the direct heating and cooling in Eq. (1), the SMCM deep convection parameterization provides downdrafts,

$$D_c = \mu\left[\frac{H_s - H_c}{\bar{Q_c}}\right]^+, \tag{7}$$

which cool and dry the boundary layer and moisten the mid-troposphere due to the evaporation and melting of stratiform precipitation that falls into a dry lower troposphere.

While further details about the implementation of the SMCM convective parametrization in CFSv2 are found in *Goswami et al.* [2017a], the SMCM temperature and moisture tendency equations are formulated below for the sake of clarity:

$$\left[\frac{\partial}{\partial t}\theta(z)\right]_{SMCM} = \begin{cases} Q_{tot}(z), & \text{if } z > h \\ Q_{tot}(z) - \frac{D_c}{h}\triangle_m\theta, & \text{if } z < h \end{cases} \tag{8}$$

$$\left[\frac{\partial}{\partial t}q(z)\right]_{SMCM} = \begin{cases} -P(z) + E(z), & \text{if } z > h \\ -P(z) - \frac{D_c}{h}\triangle_m q, & \text{if } z < h. \end{cases} \tag{9}$$

Here, $\triangle_m X$ is the difference between the middle-troposphere value and the PBL averaged value of X and $P(z)$ and $E(z)$ are the precipitation and evaporation rates, respectively, given by

$$\begin{aligned} P(z) &= Q_{tot}(z)\ Q_2(z) \\ E(z) &= \left(\delta_m(z)\frac{D_c}{H}\right)\triangle_m\theta_e, \end{aligned}$$

where $Q_2(z)$ is a vertical structure function mimicking the Yanai moisture sink profile [*Yanai et al.*, 1973] and $\delta_m(z)$ is another structure function with a bottom heavy profile used in order to realistically simulate moistening due to evaporative cooling (see Figure 4 and 5 of the Electronic Supplementary Material of *Goswami et al.* [2017a] , for the exact shapes of $Q_2(z)$ and $\delta_m(z)$ profiles). The parameter H is the height of the tropical troposphere and h is the GCM's boundary layer height.

Table 2. Parameter values (corresponds to run 129)

Reference	Parameter	Value	Remarks
Eqn 5	τ_q	144 hrs	moisture adjustment timescale
Eqn 4	τ_s	96 hrs	stratiform convection adjustment timescale
Eqn 5, 6	τ_c	240 hrs	congestus convection adjustment timescale
Eqn 7	μ	0.0125	Relative contribution of stratiform evaporative cooling to downdraft
Eqn 5, 6	γ_c	0.1	Adjustment coeff. for relative contribution of congestus to deep heating
Eqn 3	α_c	0.1	congestus adjustment coefficient
Eqn 4	α_s	0.2	stratiform adjustment coefficient
For Normalization	$CAPE0$	5000 J/kg	reference value of CAPE
	$LCAPE0$	2000 J/kg	reference value of LCAPE
	$MTD0$	5 %	reference value of MTD
	$CIN0$	5 J/kg	reference value of CIN
	$W0$	0.05 m/s	reference value of vertical velocity

In the CFSsmcm, except for replacing the SAS cumulus scheme with SMCM, the rest of that CFSv2 configuration is unchanged. For instance, CFSsmcm still uses the same shallow cumulus scheme as CFSv2 (the SMCM scheme does not have shallow convection). However, unlike the SAS scheme the SMCM implementation ignores radiative feedback from the parameterized clouds.

The details of the reference model CFSv2 are available in *Saha et al.* [2014]. We have used TRMM3b42-v7 (0.25°x 0.25°; daily) [*Huffman et al.*, 2010], outgoing long-wave radiation (OLR) from NOAA (2.5°x 2.5°; daily) [*Liebmann and Smith*, 1996] and the thermodynamical and dynamical parameters from NCEP reanalysis (2.5°x 2.5°; daily) [*Kalnay et al.*, 1996] as the observational benchmark to evaluate the model simulated climate. Indian Meteorology department (IMD) 1°x 1°rainfall data [*Rajeevan et al.*, 2006] is used an additional observational benchmark while plotting the annual cycle of rainfall over the central Indian region in Figure 4.

The parameters used in the SMCM formulation are provided in Table 2, along with their values. The values of the parameters provided in Table 2 are the ones found to be the best among 14 sets of parameter values corresponding to 14 runs made to understand the model-behaviour. Table 3 provides the different sets of parameters corresponding to the different runs considered here.

The first column of Table 3 shows the run identification numbers (ID). As can be seen from the run IDs, these 14 runs are actually a few runs selected out of 140 runs made in the process of developing the model, after completing the necessary computer coding to incorporate the SMCM in CFSv2. The reference values of CAPE, LCAPE and MTD (CAPE0, LCAPE0 and MTD0 respectively), are obtained from the CFSR [*Saha et al.*, 2010] climatology. The model is run in T126 horizontal resolution, 64 vertical levels, and a 10 minutes time step.

Table 3. Parameter values for the different CFSsmcm runs

Run ID	CAPE0	LCAPE0	MTD0	τ_q	τ_s	τ_c	α_s	τ_{30}
122	4000	1500	25	14	10	24	0.2	1
123	5000	2000	25	14	10	24	0.2	1
124	5000	2000	25	144	96	240	0.2	1
126	5000	2000	25	288	192	480	0.2	1
128	6000	3000	25	144	96	240	0.2	1
129	5000	2000	5	144	96	240	0.2	1
130	5000	2000	5	144	96	240	0.5	1
131	5000	2000	5	144	96	240	0.3	5
132	6000	3000	15	144	96	240	0.3	5
133	5000	2000	15	144	96	240	0.7	1
134	5000	2000	15	144	96	240	0.7	5
135	5000	2000	15	144	96	240	0.7	10
139	5000	2000	O=5; L=25	144	96	240	0.2	1
140	6000	3000	O=5; L=25	288	192	480	0.3	5

Determination of the adjustment timescales

Adjustment timescales measure the time over which convection brings the environment back to equilibrium. The SMCM uses three different adjustment timescales: τ_q to equilibrate moisture abundance by promoting deep convection and τ_c and τ_s are, respectively, the congestus and the stratiform convection adjustment timescales. In order to determine these timescales, the SMCM is run as a single column stochastic cloud model in standalone mode, forced by predictors coming from reanalysis. The timescales τ_q, τ_c and τ_s are calibrated by comparing the simulated precipitation with TRMM rainfall. This exercise is done for a few judiciously selected points across the globe. While the details are omitted for brevity, the optimal time-scales that are obtained during this exercise are as follows: $\tau_q = 144$ hours, $\tau_s = 96$ hours and $\tau_c = 240$ hours. While these values are adopted as the standard, here, we have also tested faster ($\tau_q = 14$ hours, $\tau_s = 10$ hours and $\tau_c = 24$ hours in runs 122 and 123) and slower ($\tau_q = 288$ hours, $\tau_s = 192$ hours and $\tau_c = 480$ hours in runs 126 and 140) adjustment time scales.

The parameters α_s and τ_{30} are chosen based on experience gained from previous studies using the SMCM in idealized settings [*Khouider et al.*, 2010; *Peters et al.*, 2013; *Deng et al.*, 2015] and the GigaLES study by *De La Chevrotière et al.* [2015].

3 Results

In this section the results from the 14 CFsmcm runs in the Table 3 are assessed and compared to a control CFSv2 simulation and to the observations. In Section 3a, we look at the mean state of the climate in terms of the daily global mean temperature and moisture at the surface and middle troposphere (500hPa). This is followed by an assessment of the climatological annual mean precipitation distribution over the globe in Section 3b. The analysis of the mean climate helps in identifying the group of parameters controlling the mean climate of the model. The middle tropospheric dryness re-normalization constant (MTD0) and the adjustment time-scales (τ_s, τ_q and τ_c in Eqns 4-6) are found to constitute this group. In Section 3c, we check the mean meridional cross-section of temperature, moisture and zonal winds, to further investigate the fidelity of the model in simulating the mean climate. In Section 3d, we indulge into assessing the model in terms of its ability to simulated the variability and organization on the intraseasonal time-scale. Here we focus more on the parameters responsible for controlling the stratiform heating in the SMCM formulation. These parameters are the stratiform adjustment coefficient (α_s in Eqn 4) and the decay time-scale of stratiform heating (τ_{30} in Table 3 last row). This is motivated by the fact that, in observations [*Schumacher et al.*, 2007; *Chattopadhyay et al.*, 2009; *Kumar et al.*, 2016] and previous SMCM studies [*Ajayamohan et al.*, 2016; *Deng et al.*, 2016, for example], stratiform heating is found to play a crucial role in organizing convection in the tropics.

3.1 Mean Temperature and Moisture

In Figure 1, we plot the global mean temperature and moisture fields at various heights, as they evolve over the 5-year simulation period, for the 14 CFSsmcm runs listed in Table 3, contrasted with the control run using the original CFSv2 model and NCEP reanalysis data (OBS). All the runs of CFSsmcm and CFSv2 are found to simulate the temperature and moisture profiles realistically though the atmosphere looks slightly cooler and drier with a tendency to further cool and dry as we proceed along time and height. Although not very severely, the cooling and drying trend continues and eventually settles down over time in the long (15 year) run (not shown here, see *Goswami et al.* [2017a,b]). At 500hPa, the CFSsmcm runs look drier compared to CFSv2, with the two runs (Runs 122 and 123) obtained with the fastest adjustment timescales, in Table 3, especially performing poorly. A notable feature of the CFSsmcm is the resilience of its mean climate, with respect to changes in parameter values, as evidenced from the overlapping temperature and moisture cycles in Fig 1. This robustness of the SMCM to changes in some key parameters, a highly desirable feature of any parameterization, is no doubted due to the fact that the scheme was designed from first principles, based on the present mean climate state. The fact that all the temperature and moisture annual means in Figure 1 are grouped together separate from the observed (reanalysis) profiles indicates that the convective parameterization is not the only factor responsible for all the climate model biases. We suspect that the systematic cooling/drying of the mid troposphere in CFSsmcm is perhaps due to the lack of radiation feedback due to the stratiform clouds [*Frenkel et al.*, 2015].

3.2 Mean Precipitation

Figure 2 shows the annual mean precipitation distributions for TRMM and the 5 year CFSv2 and CFSsmcm runs listed in Table 3. Consistent with the temperature and moisture plots in Figure 1, there are no notable differences between different CFSsmcm runs, except for the runs 122 and 123. Nonetheless, there are some noticeable deviations in terms of global mean precipitation. In Figure 3, the parameter values corresponding to different CFSsmcm runs are arranged according to increasing amount of global mean precipitation. LCAPE0 is not plotted as it's variation for the different CFSsmcm runs is similar to that of CAPE0. For a similar reason, among τ_c, τ_q and τ_s, only τ_c is plotted. Clearly, the mean precipitation (black bordered histograms) and MTD0 (the blue line) are positively correlated, in all CFSsmcm runs. It should be mentioned that, mixed MTD0 values are being used for runs 139 and 140 to take into account the land-ocean contrast. Indeed, there is no justified reason why the same MTD0 parameter value would work over both land and ocean. Runs 122 and 123 bring the mean-MTD0 correlation down. Possibly, the faster adjustment time-scales influenced the impact of MTD0 on the mean precipitation. For the adjustment time-scales obtained from the SMCM standalone calibration with TRMM and the slower ones, MTD0 appears to be the primary factor in affecting the global mean precipitation.

The impact of changing α_s (the sky blue histograms) and τ_{30} (the green histograms) values do not seem to make a large impact on the global mean precipitation. However, the organization of convection is found to be more sensitive to these parameters, as will be shown in Sub-section *d* below.

In order to assess the fidelity of the simulation of rainfall regionally, we plotted the annual cycle of precipitation at some of the major locations of active convection (Figure 4).

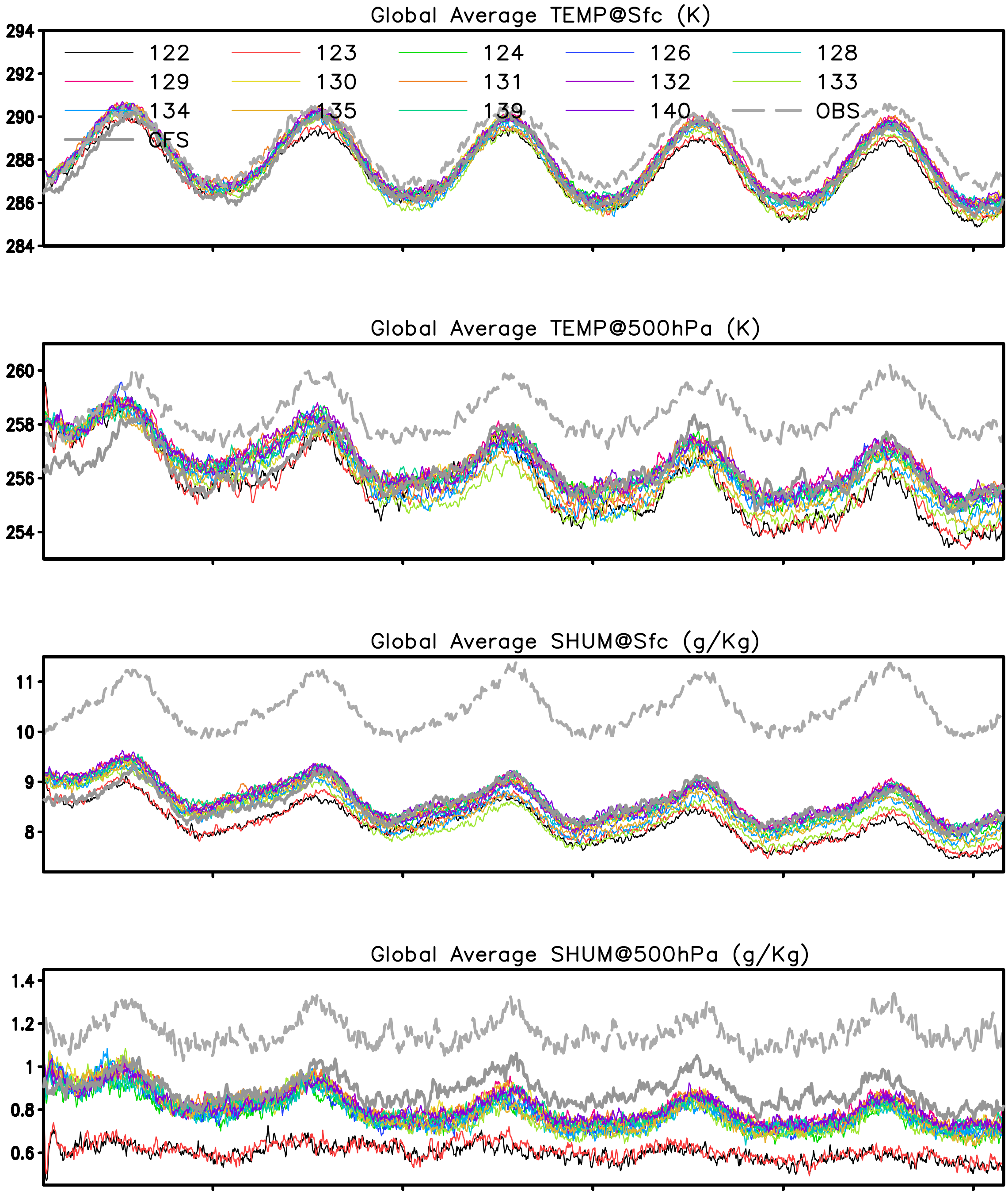

257 **Figure 1.** Global average temperature and moisture at surface and at 500hPa for the 5 years of 14 different
258 runs of CFSsmcm simulated climate compared to CFSv2 (solid grey line) and NCEP reanalysis (dashed grey
259 line).

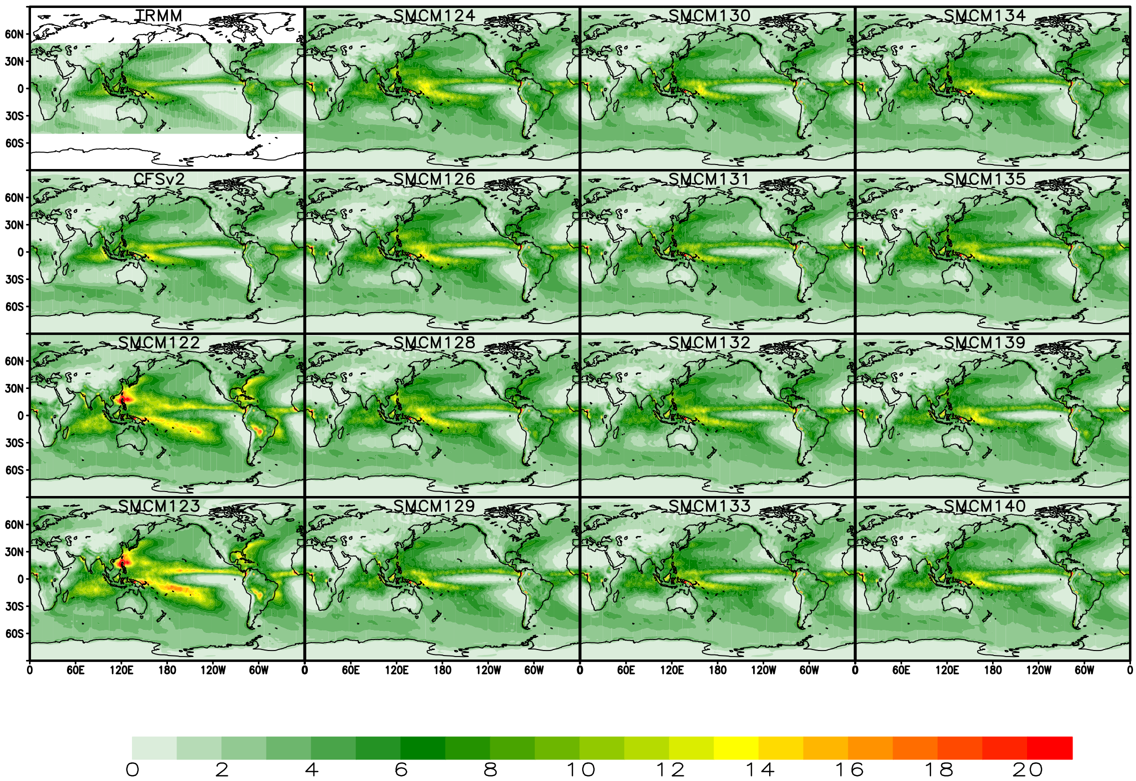

Figure 2. Climatological annual mean precipitation (mm day^{-1}) for the 5 years of 14 different runs of CFSsmcm simulated climate compared to TRMM and CFSv2.

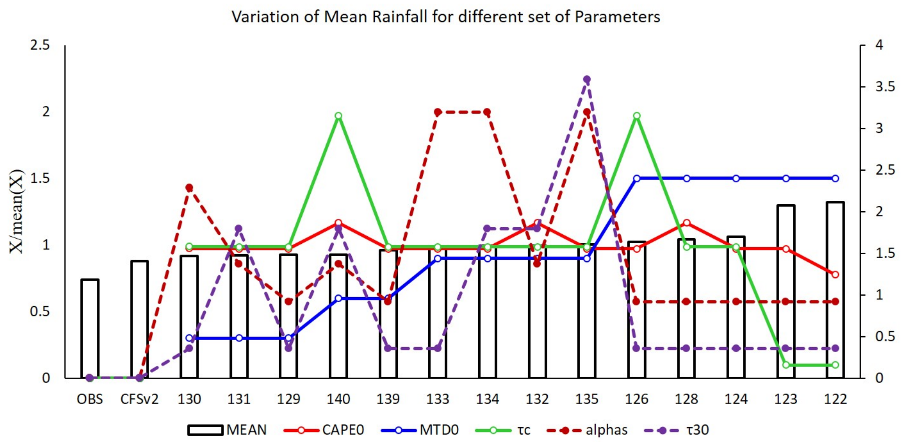

Figure 3. Variation of mean climatological rainfall (histograms) averaged over 50°S-50°N for different sets of parameters corresponding to the different CFSsmcm runs.[Note: For the runs 139 and 140, MTD0 value is calculated as = (1/4)(MTD0(over ocean)*3+MTD0(over land)*1)=(1/4)*(5*3+25*1)=10. Secondary axis is for τ_{30}.]

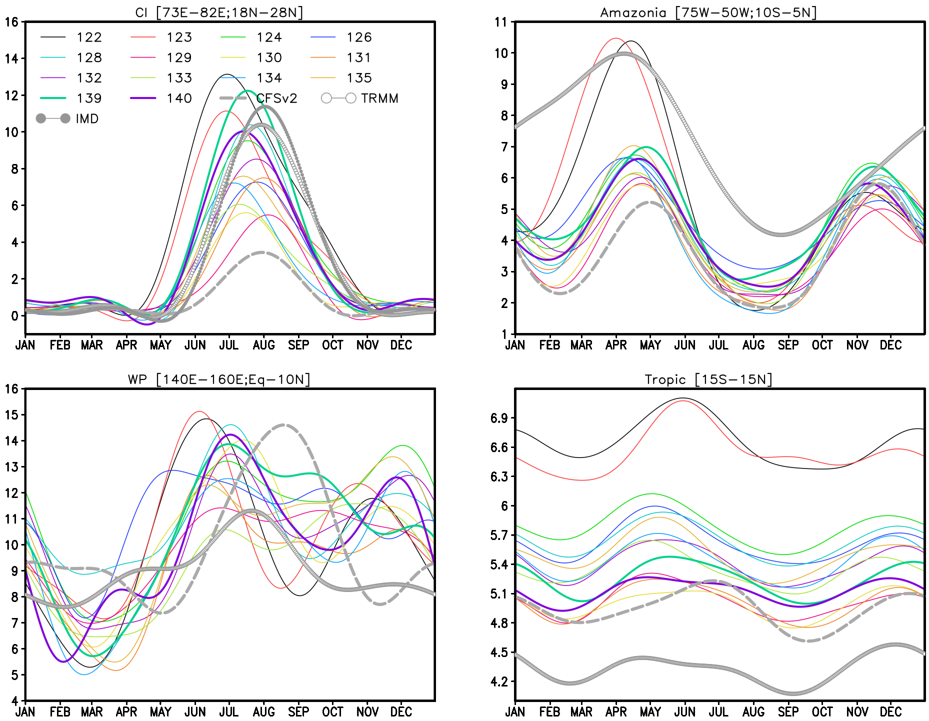

Figure 4. Annual cycle of climatological precipitation (mm day^{-1}) over 4 regions namely: Central India (CI) (73°E-82°E; 18°N-28°N), West Pacific (WP) (140°E-160°E; Eq-10°N), Amazonia (75°W-50°W; 10°S-5°N) and the entire tropics (15°S-15°N), corresponding to the different CFSsmcm runs, and for CFSv2 simulations and TRMM. Also IMD data is used for the CI region.

Over Central India (CI) and Amazonia regions, CFSv2 severely underestimates the rainfall. In fact, most state-of-the-art climate models show similar dry bias in these two locations [*Goswami and Goswami*, 2016]. Almost all the CFSsmcm runs (except 122 and 123) show a reduction in this dry bias over CI and Amazonia. However, while it is almost a tie over the Western Pacific (WP), when averaged over the entire tropics, CFSv2 is comparable with the best runs of CFSsmcm. Over the tropics, while most of the CFSsmcm runs capture the observed peak in the month of May realistically, it is almost missed in CFSv2 simulations. A closer look at Figure 4 reveals that, for land regions the CFSsmcm runs with higher MTD0 values have a smaller dry bias. Though, over the oceanic regions, and the entire tropics, it simulates too much precipitation. Similarly, for a low MTD0 value, even though the wet bias over the oceanic regions is reduced, the land regions are simulated severely dry. To address this issue, we used different MTD0 values (runs 139 and 140) for land (MTD0=25) and ocean (MTD0=5). A low MTD0 value essentially means that the middle troposphere needs to be very moist to allow deep convection. It can be seen in Figure 4 that, run 139 and 140 show relatively better annual cycles over all the regions plotted.

3.3 Mean meridional cross-sections: Temperature, Moisture, and Zonal Wind

Due to the orbital geometry of the earth, the latitudinal profiles of the zonal mean can provide valuable information about the mean climate. In Figures 5, 6, and 7, we plotted the mean meridional cross sections of temperature, moisture (specific humidity), and zonal wind, respectively, in order to further evaluate the simulations. While, in Figure 5 and 6, we have plotted the bias for temperature and moisture with respect to the NCEP reanalysis, in Figure 7, the zonal wind is plotted as is.

Before moving further, we would like to pause and caution the reader that the results in Figures 5 and 6 need to be interpreted somewhat loosely. Because the CFSv2 outputs of the dynamical variables (wind, temperature and moisture) are one-per-daily instantaneous values, taken at 00:00 UTC, while their NCEP reanalysis counterparts are daily averages, we are not comparing apples to apples per se. But a careful investigation of this issue (not shown here) was conducted by comparing two 5 year means, of the same CFSv2 runs, obtained from a 00:00 UTC one-per-daily instantaneous output, and a 3 hourly output, respectively. It is found that the difference in temperature, for example, between the two means, does not exceed 0.25°C while the differences in moisture and winds are even less-significant, relative to the major biases of CFSv2.

It is clear from Figure 5 that CFSv2 simulates a cold troposphere. This is a well documented issue of the simulated climate across generations of the Climate Forecast System framework [*Saha et al.*, 2014; *Goswami et al.*, 2015]. Further concerns of CFSv2 simulated climate are the warm bias in the upper troposphere (100-200hPa) and in the Antarctic (from the surface to about 650hPa). Barring runs 122 and 123, all CFSsmcm runs show reduced cold bias in the troposphere. More importantly, the warm bias in the upper troposphere has been reduced significantly. However, the warm bias in the Antarctic lower troposphere persists. There can be two related explanations for this. First, the SMCM parameterization is primarily designed for and based on tropical convection properties and second, the scope of any convective parameterization is naturally limited over the poles where heating and cooling is primarily driven by radiation and eddy mixing.

Figure 6 shows the zonal and time mean specific humidity bias for CFSv2 and for the 14 CFSsmcm runs. All model simulations, including CFSv2 and Runs 122 and 123, look comparable in Figure 6. However, Runs 122 and 123 are still the most biased. These two simulations are the driest in the northern hemisphere. A close evaluation reveals some differences between the different simulations near the surface, especially in the latitude band 0°-30°N. CFSv2 looks marginally drier than a few CFSsmcm runs over this latitude band. However, it should be kept in mind that these biases are computed relative to NCEP reanalyzed specific humidity field and the finer details have every possibility to look different relative

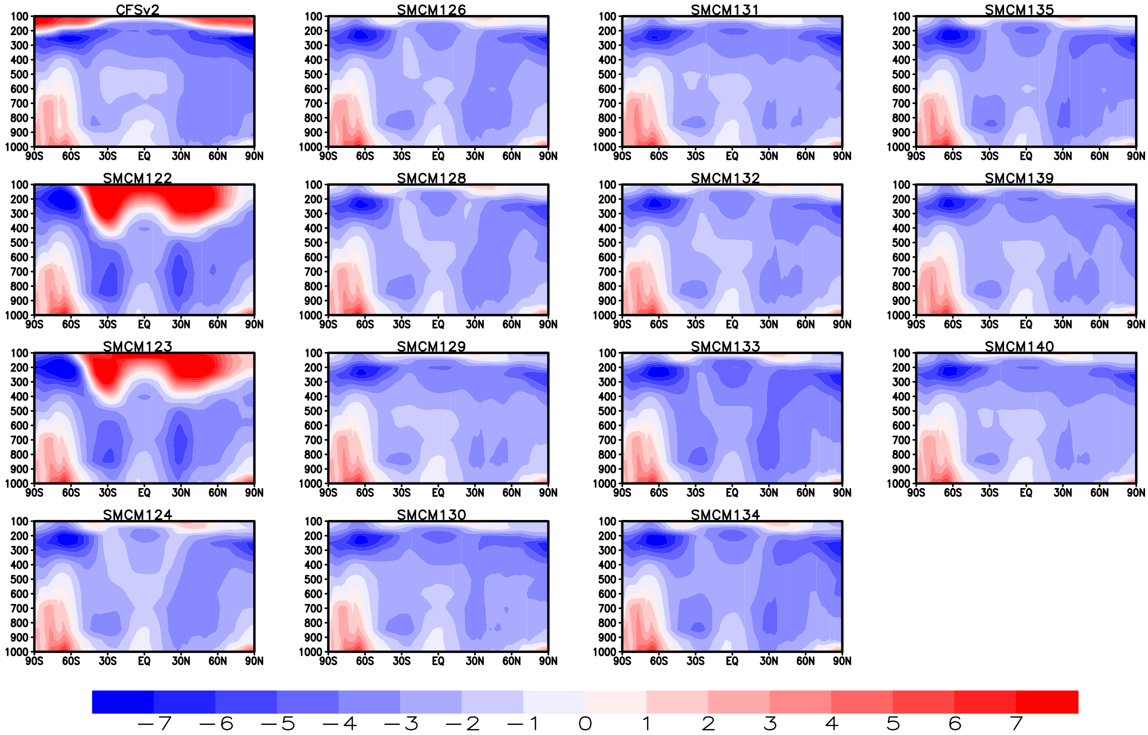

Figure 5. Bias (model simulation minus NCEP reanalysis) in the zonally-averaged temperature (Kelvin) for CFSv2 and the CFSsmcm runs.

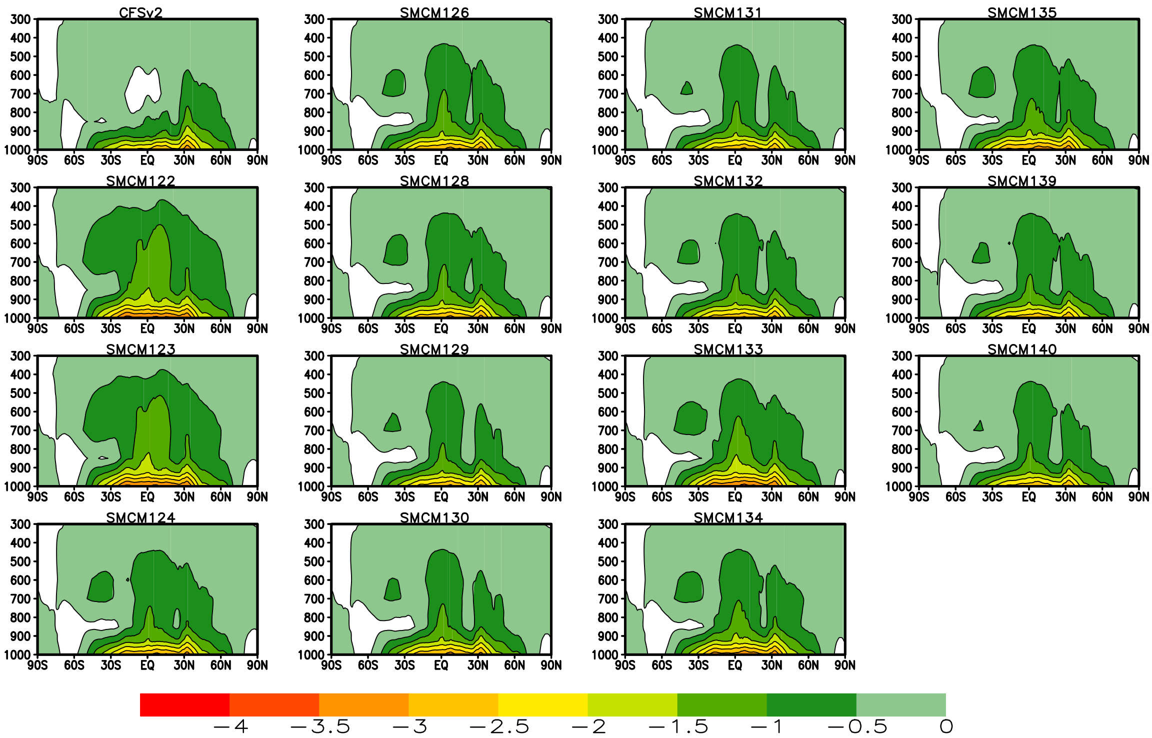

Figure 6. Bias (model simulation minus NCEP reanalysis) in the zonally-averaged specific humidity (g kg^{-1}) for CFSv2 and the CFSsmcm runs.

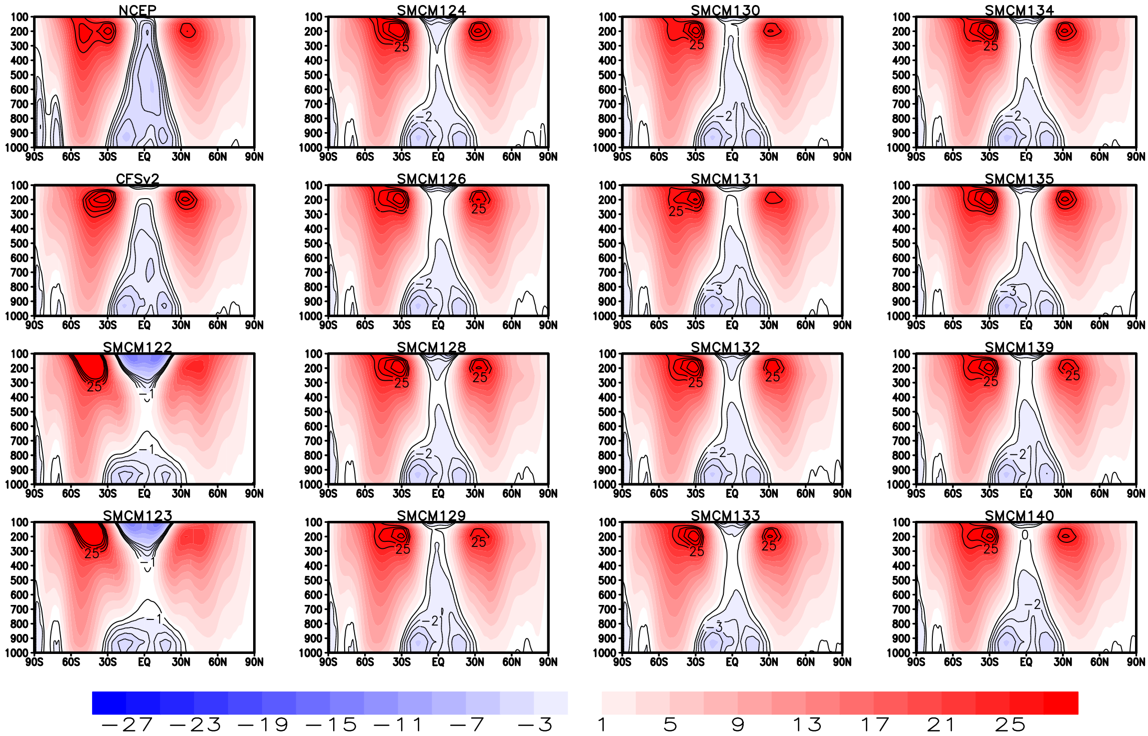

Figure 7. Mean meridional cross-section of zonal wind (m s^{-1}) for NCEP, CFSv2 and the CFSsmcm runs.

to some other reanalysis products. However, it is fair to conclude that CFSsmcm simulates a reasonably realistic moisture field near the surface, which is as good as CFSv2 simulations, if not better in some cases. (At the surface, only Runs 122,123,134,135 are worse than CFSv2).

Figure 7 shows the mean meridional cross-sections of the zonal wind. The improvement in the zonal winds is evident in the CFSsmcm simulations (especially in Runs 129, 130, 131 and 140), which is consistent with the improvements in temperature simulations seen in Figure 5. For a better visualization of the improvements of CFSsmcm simulations, the mean easterlies (negative values, with contour interval of 1ms^{-1}) including 0 ms^{-1} and the peak of the westerly jet stream (wind >25 ms^{-1}, with contour interval of 2ms^{-1}) are highlighted using additional contours over the shading. The unrealistically strong westerly jet, as indicated by the size of the 25 ms^{-1} contour loop around the location (30°N, 200 hPa), is better simulated in a few CFSsmcm simulations (prominent in runs 129, 130, 131 and 140). Also, the extend of the winter hemisphere westerly jet, located at (30°S, 200hPa), is better simulated in most of the CFSsmcm simulations (Figure for the seasonal mean meridional cross-sections of the zonal winds are not shown). The double peaked-ness of the winter hemisphere westerly jet seen in the NCEP winds is clearly missing in CFSv2; a feature all CFSsmcm runs, except runs 122 and 123, tend to capture. All the model results, including CFSv2 and CFSsmcm runs, overestimate the strength of the winter hemisphere westerly jet. A serious concern in CFSv2 simulated winds is the westerly mean flow over the equator in the upper troposphere. This equatorial superrotation implies erroneous simulation of the eddy momentum fluxes [*Saravanan*, 1993; *Biello et al.*, 2007; *Khouider et al.*, 2011]. *Kraucunas and Hartmann* [2005] argues that a proper simulation of the zonal-mean zonal winds over the equator requires the longitudinal variation of the diabatic heating to be simulated realistically. Thus, a better simulation of the zonal winds over the equator indicates a better diabatic heating in the CFSsmcm simulations. Moreover, the fact that none (except runs 122 and 123) of the

CFSsmcm runs actually indicate equatorial superrotation, is another testimony for the robustness of the SMCM formulation.

3.4 Convectively coupled equatorial waves: organization of convection

Organization is an integral part of tropical convection. The tropical atmosphere responds to the convective heating in terms of equatorial waves. These waves in turn, affect the convection by organizing it. Realistic simulation of the organization of convection implies an adequate simulation of the CCEWs. A standard metric to analyze a model's fidelity in simulating the CCEWs is the Takayabu-Wheeler-Kiladis (TWK) spectra [*Takayabu*, 1994; *Wheeler and Kiladis*, 1999]. We have plotted the symmetric and asymmetric TWK-spectra for the observed and simulated precipitation in Figure 8 and Figure 9, respectively. In the Figures 8 and 9 we have plotted the raw/background power, where background power is computed following the method of *Wheeler and Kiladis* [1999].

The features of the TWK-spectra for observation are well documented [*Wheeler and Kiladis*, 1999] and we shall avoid repeating. For CFSv2, the simulated climate underestimates the power in almost all the observed waves. In CFSsmcm, Runs 122 and 123 perform poorly. In the previous analyses presented above, we have noticed improvement in the mean climate immediately after relaxing the adjustment time-scales in 124 compared to Runs 122 and 123. However, in the case of the TWK-spectra, such dramatic improvements are not noticed. However, Run 124 provided us with a reasonable spectra to build on the tuning further. Out of the several runs performed, Run 129 simulated a decent TWK-spectra putting power in almost all the right waves although the strength of the power is underestimated. In Run 129, we had decreased the value of MTD0 to 5% in order to make the middle atmosphere wait longer until it gets much moister compared to MTD0=25% scenario in Run 124, for example, to precipitate. Noteworthy, no significant improvement in the TWK-spectra, compared to Run 124, was noted when we relaxed the adjustment time-scales (Run 126) or LCAPE0 & CAPE0 values (Run 128). As per the simulated rainfall (Figures 2 and 3 and other seasonal mean analyses not shown here), temperature (Figure 5), moisture (Figure 6) and winds (Figure 7), Run 129 looks the best among 124, 126, 127, 128 and 129. It is also the best in terms of TWK-spectra. The concern with Run 129 is that it reduces the precipitation dry bias (observed in CFSv2 simulations) only slightly. In order to explore the scope of improving the TWK-spectra further we explored the impact of changing values of α_s and τ_{30}. The rational behind this is that, a larger α_s would promote more stratiform and consequently more organization as seen in *Ajayamohan et al.* [2016] and *Deng et al.* [2016]. A recent study by *Kumar et al.* [2016], using TRMM observations, also demonstrates the role of stratiform heating in organizing the Indian summer monsoon intra-seasonal oscillations. Similarly a larger τ_{30} would keep the stratiform clouds for a longer time resulting in similar effects as a larger α_s [*Deng et al.*, 2016]. In Run 130, α_s is increased to 0.5 from 0.2 (in Run 129). And in Run 131, α_s and τ_{30} values are increased to 0.3 and 5 hrs from 0.2 and 1hr (in Run 129), respectively. Although some improvements are seen in Runs 130 and 131 in the simulated TWK-spectra, the mean precipitation got adversely effected in regions over warm oceans (figure not shown), possibly due to too many stratiform clouds. The mean rainfall in Runs 130 and 131 is still underestimated over the continents while the oceanic regions are positively biased. In Run 132, we increased the MTD0, CAPE0 and LCAPE0 parameters compared to Run 131 anticipating a balancing effect coming from increasing CAPE0 and LCAPE0 and increasing MTD0. The TWK spectra are impressive for Run 132 but the precipitation in the oceanic region is unrealistically high. We experimented with the α_s and τ_{30} values further in Runs 133, 134 and 135 keeping MTD0=15. But, one systematic behaviour of the model noted, for MTD0>5, is a wet bias over the warm oceans. Moreover for very large values of α_s and τ_{30} the TWK-spectra also deteriorated. So based on all the metrics we used to analyze the model simulations, Run 129 appeared to be the best. Hence we continued that run for 15 years. A brief overview of the last 10 of these 15 years of simulations can be found in *Goswami et al.* [2017a] and a more detailed account is reported in *Goswami et al.* [2017b].

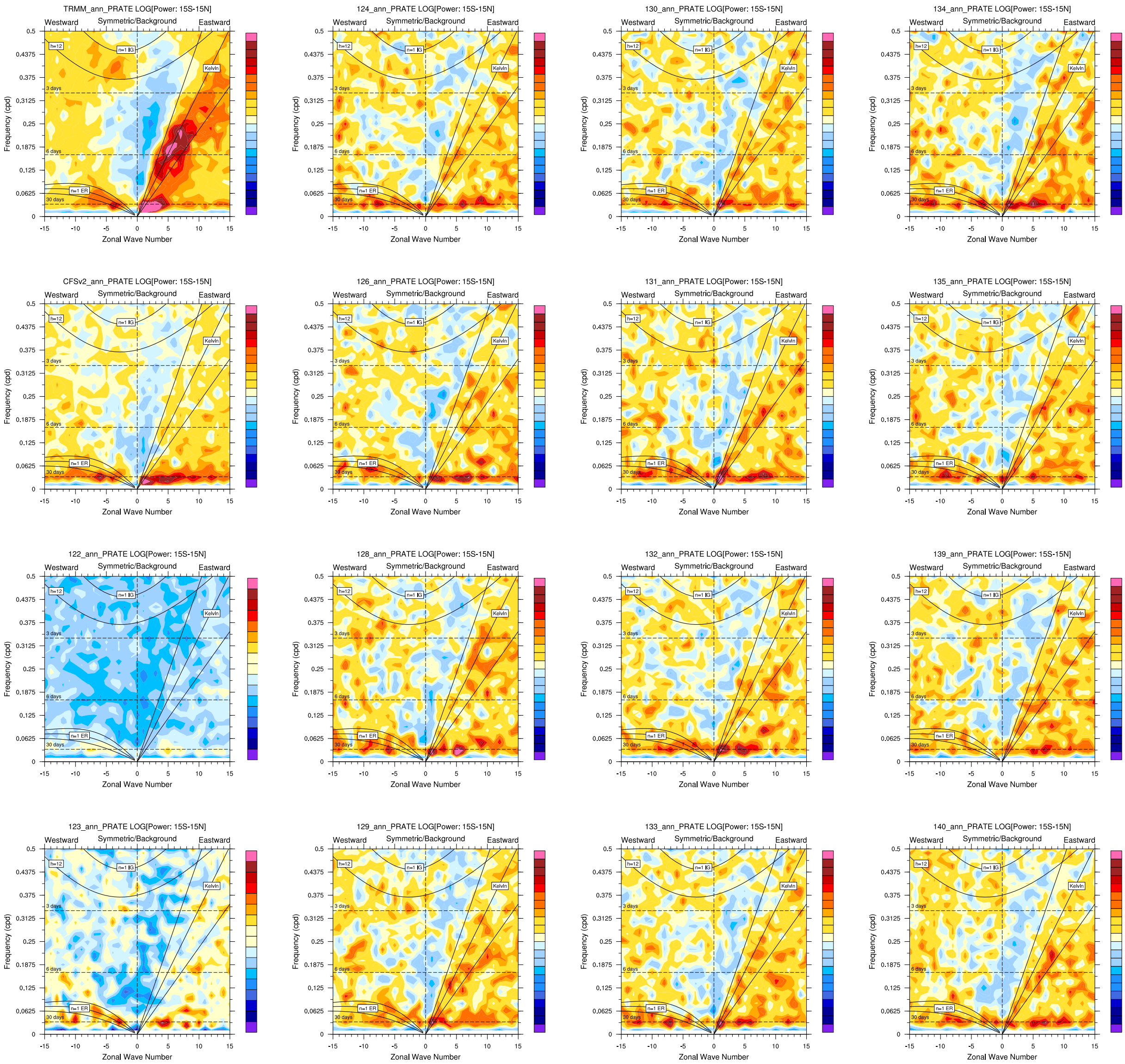

1

407 **Figure 8.** Wheeler-Kiladis spectra (symmetric component) for TRMM and simulated precipitation by
408 CFSv2 and the CFSsmcm runs.

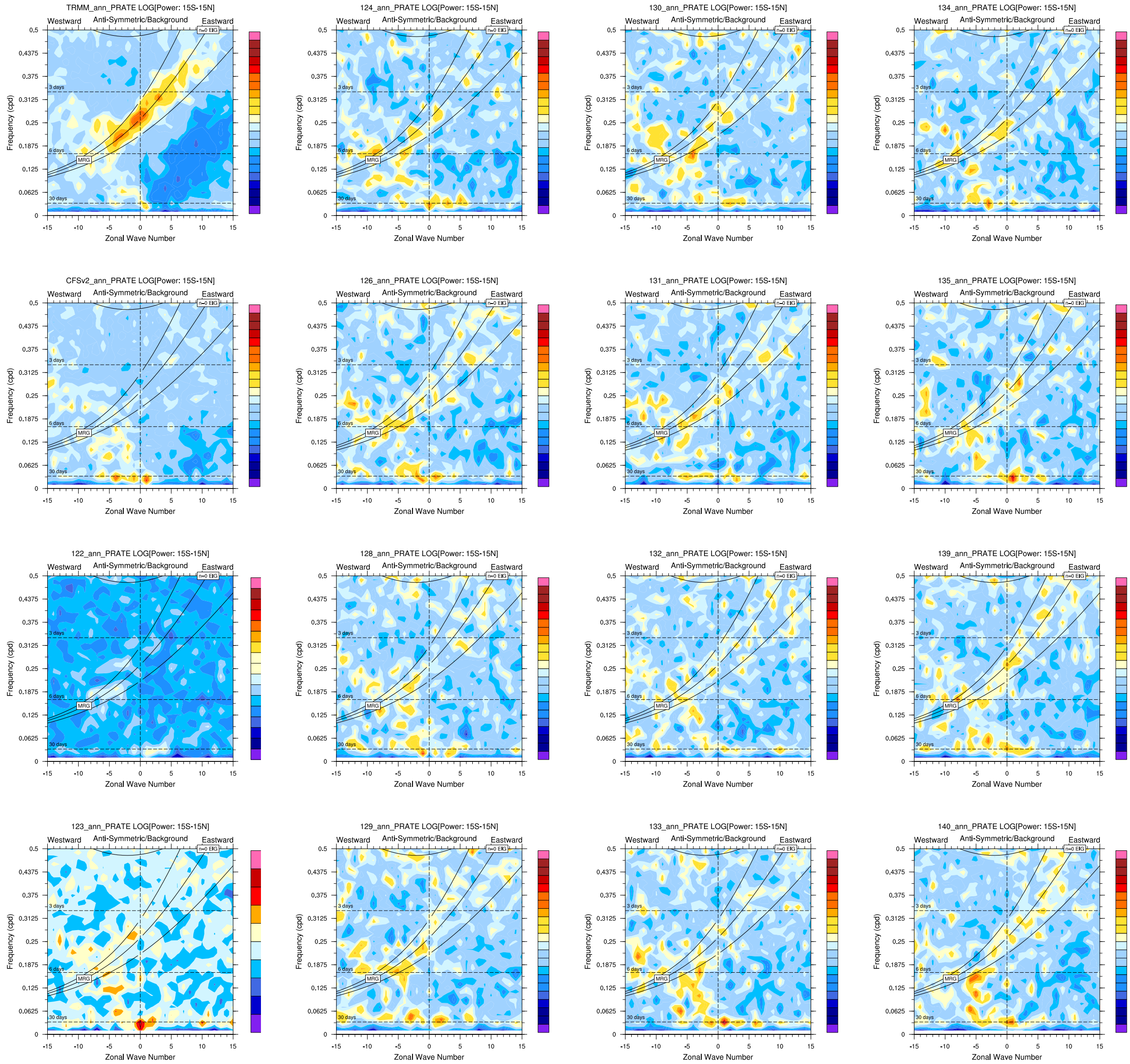

1

Figure 9. Same as Figure 8 but for the asymmetric component.

In Figure 8 the MJO power is stronger in the CFSv2 TWK-spectra compared to all the CFSsmcm runs, except Run 131. However, for a longer simulation the CFSsmcm simulates a stronger MJO as shown by [*Goswami et al.*, 2017b]. Also it is interesting to note, from a visual inspection of the Figures 8 and 9, that improvement in the asymmetric component is more prominent than the symmetric component, a feature visible for a longer simulation as well [*Goswami et al.*, 2017b]. Although, we do not have any analyses to comment on the reason behind this improvement, the key may reside in better simulation of the intertropical convergence zone (ITCZ). In a pair of recent studies, *Kiladis et al.* [2016] and *Dias and Kiladis* [2016], the authors have presented substantial evidence to relate the existence of the n=0 mixed Rossby-gravity waves and the eastward inertio-gravity waves with the split ITCZ over the west-central Pacific. Another key feature of the TWK-spectra is the improved simulation of the Kelvin waves in the SMCM implemented runs compared to the default CFSv2 model in the back drop of the findings of *Straub et al.* [2010]. While analyzing a set of CMIP3 model outputs *Straub et al.* [2010] found realistic precipitation climatology as a possible prerequisite for simulating reasonable Kelvin waves. Improvements seen in the simulation of the asymmetric TWK-spectra and the Kelvin waves is consistent with the fact that the CFSsmcm simulated mean climate is, in fact, slightly better than that of the CFSv2 [*Goswami et al.*, 2017a].

Finally, in an attempt to address the land-ocean in-homogeneity, we have simultaneously used two different MTD0 values, one for land (MTD0=25) and one for ocean (MTD0=5), in Runs 139 and 140. Run 139 is exactly the same as Run 129 except for having two MTD0 values. In Run 140, we tried to push the model to higher values for all the parameters. There is a definite improvement in the precipitation simulation in Runs 139 and 140 (Figure 4, thick green and purple lines). For convective organization, however Run 129 still looks the best.

4 Discussion and Conclusion

The implementation and calibration of the stochastic multicloud model (SMCM) convective parameterization of *Khouider et al.* [2010] in CFSv2 is presented here. In particular a thorough parameter sensitivity analysis is conducted in order to understand how the CFSsmcm coupled model responds to changes in SMCM parameters. The CFSsmcm model is found to be robust as the simulated mean climate appears to be resilient to small changes in the parameter values. Another feature noted here is that the CFSsmcm mean climate does not deteriorate while tuning the model for its variability, unlike many other state-of-the-art climate models [*Waliser et al.*, 2003; *Lin et al.*, 2006; *Kim et al.*, 2011, 2012; *Mauritsen et al.*, 2012]. In a survey of model tuning, *Hourdin et al.* [2016] states that, a specific metric targeted tuning degrades the performance of the model over some other metric.

Kim et al. [2012] reported an improvement in the simulation of the intra-seasonal variability, Madden-Julian oscillation (MJO), in a GCM by increasing the entrainment rate in the underlying mass flux-type convective parameterization. *Kim et al.* [2011] [and the relevant references therein], demonstrates that, a convection scheme can be tuned to simulate better intra-seasonal variability by making it sensitive to large scale moisture. A possible explanation, for this behaviour of the convective parameterization schemes can be found in *Lin et al.* [2006]. As discussed in *Lin et al.* [2006], a stronger moisture trigger prolongs the moisture build up for deep convection to occur. The dilemma is that the same parameterization changes lead to deterioration in the mean state. In CFSsmcm, the improvement in the simulation of intra-seasonal variability and convectively coupled equatorial waves is achieved by tuning the strength and longevity of stratiform heating. By doing so, we are also affecting the process of moisture build up leading to deep convection, which process is taken into account by the design of the SMCM through congestus moisture preconditioning [*Khouider and Majda*, 2006; *Khouider et al.*, 2010]. However, it does not deteriorate the mean climate. An investigation in the backdrop of this fundamental difference in tuning the sensitivity of the trigger to the environmental moisture between the previous studies [*Lin et al.*, 2006; *Kim* *et al.*, 2011] and the CFSsmcm formulation may provide insight to processes crucial for understanding growth of convection.

To get the mean climate right, in CFSsmcm, the most dominant parameters, are the adjustment time-scales (τ_q, τ_c and τ_s). The model's mean climate looks hugely biased for faster time-scales. However, for the time-scales obtained by calibrating the SMCM simulated precipitation, in standalone mode, with TRMM data, the mean climate looks reasonably realistic. For further prolonged adjustment time-scales, the change in the mean climate is insignificant. In a reasonably simulated mean climate, the distribution of the mean precipitation is found to be most sensitive to the mid-tropospheric dryness (MTD). The mid-tropospheric dryness has always been a key notion in the SMCM formulation [*Khouider and Majda*, 2006; *Khouider et al.*, 2010]. The reference value of MTD (MTD0) used for its own normalization, is varied to control the response of the SMCM to middle troposphere moisture. The value of MTD0 decides how moist the middle troposphere needs to be to promote deep convection: a low MTD0 value implies a moister environmental threshold and a higher value means a drier threshold. Consequently, the model yields more (less) precipitation for high (low) MTD0 values. As per our analyses, the SMCM formulation favors low value of MTD0, as otherwise the regions over the warm tropical oceans tend to precipitate too much. However, the land regions are found to be relatively lacking precipitation for low MTD0 values. Our analyses show that overall a low MTD0 value is more adequate, perhaps due to the fact that 75% of the earth surface is occupied by oceans. In an effort to find a solution to this dilemma, a variable-MTD0 value is also tried in a couple of test runs with a high MTD0 value over the continents and a low MTD0 value for the oceanic regions. Few crucial improvements are noted in these variable-MTD0 runs. The precipitation climatology is improved, in particular, the dry bias in the simulated Indian summer monsoon rainfall is significantly reduced. As a consequence, the poleward migrations of convection bands over the Indian monsoon region has improved while the TWK-spectra remain almost unchanged. This is expected, as the variable-MTD0 is primarily intended to improve the mean more than the variability. The improvements seen in these variable-MTD0 runs compared to the univalued MTD0 runs, especially compared to Run 129, are promising. However, these variable-MTD0 runs still need to be analyzed for a longer simulation.

The simulated climate variability is found to be sensitive to the parameters responsible for stratiform heating strength and lifetime. The role of stratiform heating in organizing tropical convection is well appreciated in several studies [*Schumacher et al.*, 2007; *Chattopadhyay et al.*, 2009; *Kumar et al.*, 2016]. The SMCM also, in idealized framework, captures the role of stratiform heating in organizing convection [*Ajayamohan et al.*, 2016; *Deng et al.*, 2016]. Consistent with the previous studies, the simulation of the planetary scale tropical waves is found to be sensitive to the stratiform heating and its lifetime. For quickly decaying weak stratiform heating, the organization is found to be weak. Whereas, for long-lived and strong stratiform heating the organization is much stronger. However, excessive stratiform heating is also not good as it starts deteriorating the organization (Run 135). This behaviour of the CFSsmcm is new and different from the findings of *Deng et al.* [2016] and *Ajayamohan et al.* [2016], who used an aquaplanet framework, where a long-lived and stronger stratiform heating is found to favor MJO and intra-seasonal oscillations in general while a short-lived and moderate stratiform heating promotes synoptic scale organization such as convectively coupled Kelvin waves and monsoon depressions. However no such behavior is noted in CFSsmcm, based on the TWK-spectra. Among all the 140 runs none of them were found to favor synoptic variability at the expense of MJO unlike the aquaplanet case [*Deng et al.*, 2016; *Ajayamohan et al.*, 2016]. In this coupled setting, the MJO seems to be very resilient.

The motivation behind this documentation was to evaluate the best possible set of parameters for the CFSsmcm model and gain some understanding of its sensitivity to the SMCM parameters. According to the analysis presented here the parameter regimes corresponding to Run 129 in Table 2 appears to be the most suitable when all the various metrics in sections 3a-d are weighted in. There may be some amount of uncertainty sticking to the parameter values that are found to be the most suitable but the model's resistance to slight changes in the parameter values makes this uncertainty insignificant. Nevertheless, as the model evolves further, it can be tuned more. For now, Run 129 is run for 15 years and the simulated climate is analyzed for the planetary-scale organization of convection *Goswami et al.* [2017a] and a more detailed account is reported in *Goswami et al.* [2017b].

Acknowledgments

The research of BK is partially funded by a grant from the Government of India through the National Monsoon Mission (NMM) and a discovery grant from the Canadian Natural and Sciences and Engineering Research Council. BBG is a post doctoral fellow through BK's NMM grant. TRMM3b42-v7 data is obtained from http://disc.gsfc.nasa.gov/datacollection/TRMM_3B42_Daily_7.html. NOAA OLR data is obtained from ftp://ftp.cdc.noaa.gov/Datasets/interp_OLR/olr.day.mean.nc. The NCEP reanalyses product is obtained from http://www.esrl.noaa.gov/psd/data/gridded/data.ncep.reanalysis.html. CFSR data for constructing the background for SMCM is obtained from http://rda.ucar.edu/datasets/ds093.2/.

References

Ajayamohan, R. S., B. Khouider, A. J. Majda, and Q. Deng (2016), Role of stratiform heating on the organization of convection over the monsoon trough, *Clim. Dyn.*, pp. 1–20, doi:10.1007/s00382-016-3033-7.

Arakawa, A., and W. H. Schubert (1974), Interaction of a cumulus cloud ensemble with the large-scale environment, Part I, *J. Atmos. Sci.*, *31*(3), 674–701, doi:10.1175/1520-0469(1974)031<0674:IOACCE>2.0.CO;2.

Biello, J. A., A. J. Majda, and M. W. Moncrieff (2007), Meridional momentum flux and superrotation in the multiscale IPESD MJO model, *J. Atmos. Sci.*, *64*(5), 1636–1651.

Buizza, R., M. Milleer, and T. N. Palmer (1999), Stochastic representation of model uncertainties in the ECMWF ensemble prediction system, *Q. J. R. Meteorolog. Soc.*, *125*(560), 2887–2908, doi:10.1002/qj.49712556006.

Chattopadhyay, R., B. N. Goswami, A. K. Sahai, and K. Fraedrich (2009), Role of stratiform rainfall in modifying the northward propagation of monsoon intraseasonal oscillation, *J. Geophys. Res. Atmos.*, *114*(D19), doi:10.1029/2009JD011869.

Davini, P., J. von Hardenberg, S. Corti, H. M. Christensen, S. Juricke, A. Subramanian, P. A. G. Watson, A. Weisheimer, and T. N. Palmer (2016), Climate SPHINX: evaluating the impact of resolution and stochastic physics parameterisations in climate simulations, *Geosci. Model Dev. Discuss.*, *2016*, 1–29, doi:10.5194/gmd-2016-115.

De La Chevrotière, M., and B. Khouider (2017), A zonally symmetric model for the monsoon-Hadley circulation with stochastic convective forcing, *Theor. Comput. Fluid Dyn.*, *31*(1), 89–110, doi:10.1007/s00162-016-0407-8.

De La Chevrotière, M., Michèle, B. Khouider, and A. Majda (2015), Stochasticity of convection in Giga-LES data, *Clim. Dyn.*, *47*(5), 1845–1861, doi:10.1007/s00382-015-2936-z.

Deng, Q., B. Khouider, and A. J. Majda (2015), The MJO in a coarse-resolution GCM with a stochastic multicloud parameterization, *J. Atmos. Sci.*, *72*(1), 55–74, doi:10.1175/JAS-D-14-0120.1.

Deng, Q., B. Khouider, A. J. Majda, and R. S. Ajayamohan (2016), Effect of stratiform heating on the planetary-scale organization of tropical convection, *J. Atmos. Sci.*, *73*(1), 371–392, doi:10.1175/JAS-D-15-0178.1.

Dias, J., and G. N. Kiladis (2016), The relationship between equatorial mixed rossby–gravity and eastward inertio-gravity waves. Part II, *J. Atmos. Sci.*, *73*(5), 2147–2163, doi:10.1175/JAS-D-15-0231.1.

Dorrestijn, J., D. Crommelin, J. Biello, and S. Böing (2013a), A data-driven multi-cloud model for stochastic parametrization of deep convection, *Philos. Trans. R. Soc. London, Ser. A*, *371*(1991), 20120,374.

Dorrestijn, J., D. T. Crommelin, A. P. Siebesma, and H. J. Jonker (2013b), Stochastic parameterization of shallow cumulus convection estimated from high-resolution model data, *Theor. Comput. Fluid Dyn.*, *27*(1-2), 133–148.

Dorrestijn, J., D. T. Crommelin, A. P. Siebesma, H. J. Jonker, and C. Jakob (2015), Stochastic parameterization of convective area fractions with a multicloud model inferred from observational data, *J. Atmos. Sci.*, *72*(2), 854–869.

Dorrestijn, J., D. T. Crommelin, A. P. Siebesma, H. J. Jonker, and F. Selten (2016), Stochastic convection parameterization with Markov Chains in an intermediate-complexity GCM, *J. Atmos. Sci.*, *73*(3), 1367–1382.

Frenkel, Y., A. J. Majda, and B. Khouider (2012), Using the stochastic multicloud model to improve tropical convective parameterization: A paradigm example, *J. Atmos. Sci.*, *69*(3), 1080–1105, doi:10.1175/JAS-D-11-0148.1.

Frenkel, Y., A. J. Majda, and B. Khouider (2013), Stochastic and deterministic multicloud parameterizations for tropical convection, *Clim. Dyn.*, *41*(5-6), 1527–1551, doi:10.1007/s00382-013-1678-z.

Frenkel, Y., A. J. Majda, and S. N. Stechmann (2015), Cloud-radiation feedback and atmosphere-ocean coupling in a stochastic multicloud model, *Dyn. Atmos. Oceans*, *71*, 35–55, doi:10.1016/j.dynatmoce.2015.05.003.

Goswami, B. B., and B. N. Goswami (2016), A road map for improving dry-bias in simulating the south Asian monsoon precipitation by climate models, *Clim. Dyn.*, *0*(0), null, doi:10.1007/s00382-016-3439-2.

Goswami, B. B., R. P. M. Krishna, P. Mukhopadhyay, M. Khairoutdinov, and B. N. Goswami (2015), Simulation of the Indian summer monsoon in the superparameterized Climate Forecast System version 2: Preliminary results, *J. Clim.*, *28*(22), 8988–9012, doi:10.1175/JCLI-D-14-00607.1.

Goswami, B. B., B. Khouider, R. P. M. Krishna, P. Mukhopadhyay, and A. J. Majda (2017a), Improving synoptic and intra-seasonal variability in CFSv2 via stochastic representation of organized convection, *Geophys. Res. Lett.*, *44*(2), 1104–1113, doi:10.1002/2016GL071542.

Goswami, B. B., B. Khouider, R. P. M. Krishna, P. Mukhopadhyay, and A. J. Majda (2017b), Improved tropical modes of variability in the Climate Forecast System model (version 2) via a stochastic multicloud model, *J. Atmos. Sci.*, doi:submitted.

Hourdin, F., T. Mauritsen, A. Gettelman, J.-C. Golaz, V. Balaji, Q. Duan, D. Folini, D. Ji, D. Klocke, Y. Qian, F. Rauser, C. Rio, L. Tomassini, M. Watanabe, and D. Williamson (2016), The art and science of climate model tuning, *Bull. Am. Meteorol. Soc.*, *0*(0), null, doi:10.1175/BAMS-D-15-00135.1.

Huffman, G. J., R. F. Adler, D. T. Bolvin, and E. J. Nelkin (2010), The TRMM multi-satellite precipitation analysis (TMPA), in *Satellite Rainfall Applications for Surface Hydrology*, pp. 3–22, Springer, doi:10.1007/978-90-481-2915-7_1.

Johnson, R. H., T. M. Rickenbach, S. A. Rutledge, P. E. Ciesielski, and W. H. Schubert (1999), Trimodal characteristics of tropical convection, *J. Clim.*, *12*(8), 2397–2418.

Kalnay, E., M. Kanamitsu, R. Kistler, W. Collins, D. Deaven, L. Gandin, M. Iredell, S. Saha, G. White, J. Woollen, Y. Zhu, A. Leetmaa, R. Reynolds, M. Chelliah, W. Ebisuzaki, W. Higgins, J. Janowiak, K. C. Mo, C. Ropelewski, J. Wang, R. Jenne, and D. Joseph (1996), The NCEP/NCAR 40-Year reanalysis project, *Bull. Am. Meteorol. Soc.*, *77*(3), 437–471, doi:10.1175/1520-0477(1996)077<0437:TNYRP>2.0.CO;2.

Khairoutdinov, M. F., S. K. Krueger, C.-H. Moeng, P. A. Bogenschutz, and D. A. Randall (2009), Large-eddy simulation of maritime deep tropical convection, *J. Adv. Model. Earth Syst.*, *1*(4).

Khouider, B., and A. J. Majda (2006), A simple multicloud parameterization for convectively coupled tropical waves. Part I: Linear analysis, *J. Atmos. Sci.*, *63*(4), 1308–1323, doi:10.1175/JAS3677.1.

Khouider, B., and A. J. Majda (2008), Multicloud models for organized tropical convection: Enhanced congestus heating, *J. Atmos. Sci.*, *65*(3), 895–914, doi:10.1175/2007JAS2408.1.

Khouider, B., A. J. Majda, and M. A. Katsoulakis (2003), Coarse-grained stochastic models for tropical convection and climate., *Proc. Natl. Acad. Sci. U.S.A.*, *100*(21), 11,941–6, doi:10.1073/pnas.1634951100.

Khouider, B., J. Biello, and A. J. Majda (2010), A stochastic multicloud model for tropical convection, *Commun. Math. Sci.*, *8*(1), 187–216.

Khouider, B., A. St-Cyr, A. J. Majda, and J. Tribbia (2011), The MJO and convectively coupled waves in a coarse-resolution GCM with a simple multicloud parameterization, *J. Atmos. Sci.*, *68*(2), 240–264, doi:10.1175/2010JAS3443.1.

Kiladis, G. N., J. Dias, and M. Gehne (2016), The relationship between equatorial mixed rossby–gravity and eastward inertio-gravity waves. Part I, *J. Atmos. Sci.*, *73*(5), 2123–2145, doi:10.1175/JAS-D-15-0230.1.

Kim, D., A. H. Sobel, E. D. Maloney, D. M. Frierson, and I.-S. Kang (2011), A systematic relationship between intraseasonal variability and mean state bias in AGCM simulations, *J. Clim.*, *24*(21), 5506–5520.

Kim, D., A. H. Sobel, A. D. Del Genio, Y. Chen, S. J. Camargo, M.-S. Yao, M. Kelley, and L. Nazarenko (2012), The tropical subseasonal variability simulated in the NASA GISS general circulation model, *J. Clim.*, *25*(13), 4641–4659.

Kraucunas, I., and D. L. Hartmann (2005), Equatorial superrotation and the factors controlling the zonal-mean zonal winds in the tropical upper troposphere, *J. Atmos. Sci.*, *62*(2), 371–389, doi:10.1175/JAS-3365.1.

Kumar, S., A. Arora, R. Chattopadhyay, A. Hazra, S. A. Rao, and B. N. Goswami (2016), Seminal role of stratiform clouds in large-scale aggregation of tropical rain in boreal summer monsoon intraseasonal oscillations, *Clim. Dyn.*, pp. 1–17, doi:10.1007/s00382-016-3124-5.

Liebmann, B., and C. Smith (1996), Description of a complete (Interpolated) outgoing longwave radiation dataset., *Bull. Am. Meteorol. Soc.*, *77*, 1275–1277.

Lin, J.-L., G. N. Kiladis, B. E. Mapes, K. M. Weickmann, K. R. Sperber, W. Lin, M. C. Wheeler, S. D. Schubert, A. Del Genio, L. J. Donner, et al. (2006), Tropical intraseasonal variability in 14 IPCC AR4 climate models. Part I: Convective signals, *J. Clim.*, *19*(12), 2665–2690.

Lin, J. W.-B., and J. D. Neelin (2000), Influence of a stochastic moist convective parameterization on tropical climate variability, *Geophys. Res. Lett.*, *27*(22), 3691–3694, doi:10.1029/2000GL011964.

Lin, J. W.-B., and J. D. Neelin (2002), Considerations for stochastic convective parameterization, *J. Atmos. Sci.*, *59*(5), 959–975, doi:10.1175/1520-0469(2002)059<0959:CFSCP>2.0.CO;2.

Lin, J. W.-B., and J. D. Neelin (2003), Toward stochastic deep convective parameterization in general circulation models, *Geophys. Res. Lett.*, *30*(4), doi:10.1029/2002GL016203.

Lin, X., and R. H. Johnson (1996), Heating, moistening, and rainfall over the Western Pacific warm pool during TOGA COARE, *J. Atmos. Sci.*, *53*(22), 3367–3383, doi:10.1175/1520-0469(1996)053<3367:HMAROT>2.0.CO;2.

Majda, A. J., and B. Khouider (2002), Stochastic and mesoscopic models for tropical convection, *Proc. Natl. Acad. Sci. U.S.A.*, *99*(3), 1123–1128, doi:10.1073/pnas.032663199.

Mapes, B., S. Tulich, J. Lin, and P. Zuidema (2006), The mesoscale convection life cycle: Building block or prototype for large-scale tropical waves?, *Dyn. Atmos. Oceans*, *42*(1-4), 3–29, doi:10.1016/j.dynatmoce.2006.03.003.

Mauritsen, T., B. Stevens, E. Roeckner, T. Crueger, M. Esch, M. Giorgetta, H. Haak, J. Jungclaus, D. Klocke, D. Matei, et al. (2012), Tuning the climate of a global model, *J. Adv. Model. Earth Syst.*, *4*(3).

Moncrieff, M. W., D. E. Waliser, M. J. Miller, M. A. Shapiro, G. R. Asrar, and J. Caughey (2012), Multiscale convective organization and the YOTC virtual global field campaign, *Bull. Am. Meteorol. Soc.*, *93*(8), 1171–1187, doi:10.1175/BAMS-D-11-00233.1.

Palmer, T. (1996), On parameterizing scales that are only somewhat smaller than the smallest resolved scales, with application to convection and orography, in *Workshop on New In-*

sights and Approaches to Convective Parametrization, 4-7 November 1996, pp. 328–337, ECMWF, ECMWF, Shinfield Park, Reading.

Palmer, T. N. (2001), A nonlinear dynamical perspective on model error: A proposal for non-local stochastic-dynamic parametrization in weather and climate prediction models, *Q. J. R. Meteorolog. Soc.*, *127*(572), 279–304, doi:10.1002/qj.49712757202.

Pan, H., and W.-S. Wu (1995), Implementing a mass flux convection parameterization package for the NMC medium-range forecast model, *NMC office note*, *409*(40), 20–233.

Pattanaik, S., S. Abhilash, S. De, A. K. Sahai, R. Phani, and B. N. Goswami (2013), Influence of convective parameterization on the systematic errors of Climate Forecast System (CFS) model over the Indian monsoon region from an extended range forecast perspective, *Clim. Dyn.*, *41*(2), 341–365, doi:10.1007/s00382-013-1662-7.

Peters, K., C. Jakob, L. Davies, B. Khouider, and A. J. Majda (2013), Stochastic behavior of tropical convection in observations and a multicloud model, *J. Atmos. Sci.*, *70*(11), 3556–3575, doi:10.1175/JAS-D-13-031.1.

Peters, K., T. Crueger, C. Jakob, and B. Möbis (2017), Improved MJO-simulation in ECHAM6.3 by coupling a stochastic multicloud model to the convection scheme, *J. Adv. Model. Earth Syst.*, doi:10.1002/2016MS000809.

Plant, R. S., and G. C. Craig (2008), A stochastic parameterization for deep convection based on equilibrium statistics, *J. Atmos. Sci.*, *65*, 87–105, doi: doi:10.1175/2007JAS2263.1.

Rajeevan, M., J. Bhate, J. Kale, and B. Lal (2006), High resolution daily gridded rainfall data for the indian region: Analysis of break and active, *Current Science*, *91*(3).

Saha, S., S. Moorthi, H.-L. Pan, X. Wu, J. Wang, S. Nadiga, P. Tripp, R. Kistler, J. Woollen, D. Behringer, H. Liu, D. Stokes, R. Grumbine, G. Gayno, J. Wang, Y.-T. Hou, H.-Y. Chuang, H.-M. H. Juang, J. Sela, M. Iredell, R. Treadon, D. Kleist, P. Van Delst, D. Keyser, J. Derber, M. Ek, J. Meng, H. Wei, R. Yang, S. Lord, H. Van Den Dool, A. Kumar, W. Wang, C. Long, M. Chelliah, Y. Xue, B. Huang, J.-K. Schemm, W. Ebisuzaki, R. Lin, P. Xie, M. Chen, S. Zhou, W. Higgins, C.-Z. Zou, Q. Liu, Y. Chen, Y. Han, L. Cucurull, R. W. Reynolds, G. Rutledge, and M. Goldberg (2010), The NCEP Climate Forecast System reanalysis, *Bull. Am. Meteorol. Soc.*, *91*(8), 1015–1057, doi: 10.1175/2010BAMS3001.1.

Saha, S., S. Moorthi, X. Wu, J. Wang, S. Nadiga, P. Tripp, D. Behringer, Y.-T. Hou, H.-y. Chuang, M. Iredell, M. Ek, J. Meng, R. Yang, M. P. Mendez, H. van den Dool, Q. Zhang, W. Wang, M. Chen, and E. Becker (2014), The NCEP Climate Forecast System version 2, *J. Clim.*, *27*(6), 2185–2208, doi:10.1175/JCLI-D-12-00823.1.

Saravanan, R. (1993), Equatorial superrotation and maintenance of the general circulation in two-level models, *J. Atmos. Sci.*, *50*(9), 1211–1227.

Schumacher, C., M. H. Zhang, and P. E. Ciesielski (2007), Heating structures of the TRMM field campaigns, *J. Atmos. Sci.*, *64*(7), 2593–2610, doi:10.1175/JAS3938.1.

Straub, K. H., P. T. Haertel, and G. N. Kiladis (2010), An analysis of convectively coupled kelvin waves in 20 WCRP CMIP3 global coupled climate models, *J. Clim.*, *23*(11), 3031–3056, doi:10.1175/2009JCLI3422.1.

Takayabu, Y. N. (1994), Large-scale cloud disturbances associated with equatorial waves. Part II: Westward-propagating inertio-gravity waves, *J. Meteorol. Soc. Jpn.*, *72*(3), 451–465.

Teixeira, J., and C. A. Reynolds (2008), Stochastic nature of physical parameterizations in ensemble prediction: A stochastic convection approach, *Mon. Weather Rev.*, *136*(2), 483–496, doi:10.1175/2007MWR1870.1.

Waliser, D., K. Jin, I.-S. Kang, W. Stern, S. Schubert, M. Wu, K.-M. Lau, M.-I. Lee, V. Krishnamurthy, A. Kitoh, et al. (2003), AGCM simulations of intraseasonal variability associated with the Asian summer monsoon, *Clim. Dyn.*, *21*(5-6), 423–446.

Wheeler, M., and G. N. Kiladis (1999), Convectively coupled equatorial waves: Analysis of clouds and temperature in the wavenumber-frequency domain, *J. Atmos. Sci.*, *56*(3), 374–399, doi:10.1175/1520-0469(1999)056<0374:CCEWAO>2.0.CO;2.

Yanai, M., S. Esbensen, and J.-H. Chu (1973), Determination of bulk properties of tropical cloud clusters from large-scale heat and moisture budgets, *J. Atmos. Sci.*, *30*(4), 611–627.

References

Ajayamohan, R. S., B. Khouider, A. J. Majda, and Q. Deng (2016), Role of stratiform heating on the organization of convection over the monsoon trough, *Clim. Dyn.*, pp. 1–20, doi: 10.1007/s00382-016-3033-7.

Arakawa, A., and W. H. Schubert (1974), Interaction of a cumulus cloud ensemble with the large-scale environment, Part I, *J. Atmos. Sci.*, *31*(3), 674–701, doi:10.1175/1520-0469(1974)031<0674:IOACCE>2.0.CO;2.

Biello, J. A., A. J. Majda, and M. W. Moncrieff (2007), Meridional momentum flux and superrotation in the multiscale IPESD MJO model, *J. Atmos. Sci.*, *64*(5), 1636–1651.

Buizza, R., M. Milleer, and T. N. Palmer (1999), Stochastic representation of model uncertainties in the ECMWF ensemble prediction system, *Q. J. R. Meteorolog. Soc.*, *125*(560), 2887–2908, doi:10.1002/qj.49712556006.

Chattopadhyay, R., B. N. Goswami, A. K. Sahai, and K. Fraedrich (2009), Role of stratiform rainfall in modifying the northward propagation of monsoon intraseasonal oscillation, *J. Geophys. Res. Atmos.*, *114*(D19), doi:10.1029/2009JD011869.

Davini, P., J. von Hardenberg, S. Corti, H. M. Christensen, S. Juricke, A. Subramanian, P. A. G. Watson, A. Weisheimer, and T. N. Palmer (2016), Climate SPHINX: evaluating the impact of resolution and stochastic physics parameterisations in climate simulations, *Geosci. Model Dev. Discuss.*, *2016*, 1–29, doi:10.5194/gmd-2016-115.

De La Chevrotière, M., and B. Khouider (2017), A zonally symmetric model for the monsoon-Hadley circulation with stochastic convective forcing, *Theor. Comput. Fluid Dyn.*, *31*(1), 89–110, doi:10.1007/s00162-016-0407-8.

De La Chevrotière, M., Michèle, B. Khouider, and A. Majda (2015), Stochasticity of convection in Giga-LES data, *Clim. Dyn.*, *47*(5), 1845–1861, doi:10.1007/s00382-015-2936-z.

Deng, Q., B. Khouider, and A. J. Majda (2015), The MJO in a coarse-resolution GCM with a stochastic multicloud parameterization, *J. Atmos. Sci.*, *72*(1), 55–74, doi:10.1175/JAS-D-14-0120.1.

Deng, Q., B. Khouider, A. J. Majda, and R. S. Ajayamohan (2016), Effect of stratiform heating on the planetary-scale organization of tropical convection, *J. Atmos. Sci.*, *73*(1), 371–392, doi:10.1175/JAS-D-15-0178.1.

Dias, J., and G. N. Kiladis (2016), The relationship between equatorial mixed rossbyâ€“gravity and eastward inertio-gravity waves. Part II, *J. Atmos. Sci.*, *73*(5), 2147–2163, doi:10.1175/JAS-D-15-0231.1.

Dorrestijn, J., D. Crommelin, J. Biello, and S. Böing (2013a), A data-driven multi-cloud model for stochastic parametrization of deep convection, *Philos. Trans. R. Soc. London, Ser. A*, *371*(1991), 20120,374.

Dorrestijn, J., D. T. Crommelin, A. P. Siebesma, and H. J. Jonker (2013b), Stochastic parameterization of shallow cumulus convection estimated from high-resolution model data, *Theor. Comput. Fluid Dyn.*, *27*(1-2), 133–148.

Dorrestijn, J., D. T. Crommelin, A. P. Siebesma, H. J. Jonker, and C. Jakob (2015), Stochastic parameterization of convective area fractions with a multicloud model inferred from observational data, *J. Atmos. Sci.*, *72*(2), 854–869.

Dorrestijn, J., D. T. Crommelin, A. P. Siebesma, H. J. Jonker, and F. Selten (2016), Stochastic convection parameterization with Markov Chains in an intermediate-complexity GCM, *J. Atmos. Sci.*, *73*(3), 1367–1382.

Frenkel, Y., A. J. Majda, and B. Khouider (2012), Using the stochastic multicloud model to improve tropical convective parameterization: A paradigm example, *J. Atmos. Sci.*, *69*(3), 1080–1105, doi:10.1175/JAS-D-11-0148.1.

Frenkel, Y., A. J. Majda, and B. Khouider (2013), Stochastic and deterministic multicloud parameterizations for tropical convection, *Clim. Dyn.*, *41*(5-6), 1527–1551, doi:10.1007/s00382-013-1678-z.

Frenkel, Y., A. J. Majda, and S. N. Stechmann (2015), Cloud-radiation feedback and atmosphere-ocean coupling in a stochastic multicloud model, *Dyn. Atmos. Oceans*, *71*, 35–55, doi:10.1016/j.dynatmoce.2015.05.003.

Goswami, B. B., and B. N. Goswami (2016), A road map for improving dry-bias in simulating the south Asian monsoon precipitation by climate models, *Clim. Dyn.*, *0*(0), null, doi:10.1007/s00382-016-3439-2.

Goswami, B. B., R. P. M. Krishna, P. Mukhopadhyay, M. Khairoutdinov, and B. N. Goswami (2015), Simulation of the Indian summer monsoon in the superparameterized Climate Forecast System version 2: Preliminary results, *J. Clim.*, *28*(22), 8988–9012, doi:10.1175/JCLI-D-14-00607.1.

Goswami, B. B., B. Khouider, R. P. M. Krishna, P. Mukhopadhyay, and A. J. Majda (2017a), Improving synoptic and intra-seasonal variability in CFSv2 via stochastic representation of organized convection, *Geophys. Res. Lett.*, *44*(2), 1104–1113, doi:10.1002/2016GL071542.

Goswami, B. B., B. Khouider, R. P. M. Krishna, P. Mukhopadhyay, and A. J. Majda (2017b), Improved tropical modes of variability in the Climate Forecast System model (version 2) via a stochastic multicloud model, *J. Atmos. Sci.*, doi:submitted.

Hourdin, F., T. Mauritsen, A. Gettelman, J.-C. Golaz, V. Balaji, Q. Duan, D. Folini, D. Ji, D. Klocke, Y. Qian, F. Rauser, C. Rio, L. Tomassini, M. Watanabe, and D. Williamson (2016), The art and science of climate model tuning, *Bull. Am. Meteorol. Soc.*, *0*(0), null, doi:10.1175/BAMS-D-15-00135.1.

Huffman, G. J., R. F. Adler, D. T. Bolvin, and E. J. Nelkin (2010), The TRMM multi-satellite precipitation analysis (TMPA), in *Satellite Rainfall Applications for Surface Hydrology*, pp. 3–22, Springer, doi:10.1007/978-90-481-2915-7_1.

Johnson, R. H., T. M. Rickenbach, S. A. Rutledge, P. E. Ciesielski, and W. H. Schubert (1999), Trimodal characteristics of tropical convection, *J. Clim.*, *12*(8), 2397–2418.

Kalnay, E., M. Kanamitsu, R. Kistler, W. Collins, D. Deaven, L. Gandin, M. Iredell, S. Saha, G. White, J. Woollen, Y. Zhu, A. Leetmaa, R. Reynolds, M. Chelliah, W. Ebisuzaki, W. Higgins, J. Janowiak, K. C. Mo, C. Ropelewski, J. Wang, R. Jenne, and D. Joseph (1996), The NCEP/NCAR 40-Year reanalysis project, *Bull. Am. Meteorol. Soc.*, *77*(3), 437–471, doi:10.1175/1520-0477(1996)077<0437:TNYRP>2.0.CO;2.

Khairoutdinov, M. F., S. K. Krueger, C.-H. Moeng, P. A. Bogenschutz, and D. A. Randall (2009), Large-eddy simulation of maritime deep tropical convection, *J. Adv. Model. Earth Syst.*, *1*(4).

Khouider, B., and A. J. Majda (2006), A simple multicloud parameterization for convectively coupled tropical waves. Part I: Linear analysis, *J. Atmos. Sci.*, *63*(4), 1308–1323, doi:10.1175/JAS3677.1.

Khouider, B., and A. J. Majda (2008), Multicloud models for organized tropical convection: Enhanced congestus heating, *J. Atmos. Sci.*, *65*(3), 895–914, doi:10.1175/2007JAS2408.1.

Khouider, B., A. J. Majda, and M. A. Katsoulakis (2003), Coarse-grained stochastic models for tropical convection and climate., *Proc. Natl. Acad. Sci. U.S.A.*, *100*(21), 11,941–6, doi:10.1073/pnas.1634951100.

Khouider, B., J. Biello, and A. J. Majda (2010), A stochastic multicloud model for tropical convection, *Commun. Math. Sci.*, *8*(1), 187–216.

Khouider, B., A. St-Cyr, A. J. Majda, and J. Tribbia (2011), The MJO and convectively coupled waves in a coarse-resolution GCM with a simple multicloud parameterization, *J. Atmos. Sci.*, *68*(2), 240–264, doi:10.1175/2010JAS3443.1.

Kiladis, G. N., J. Dias, and M. Gehne (2016), The relationship between equatorial mixed rossbyâ€“gravity and eastward inertio-gravity waves. Part I, *J. Atmos. Sci.*, *73*(5), 2123–2145, doi:10.1175/JAS-D-15-0230.1.

Kim, D., A. H. Sobel, E. D. Maloney, D. M. Frierson, and I.-S. Kang (2011), A systematic relationship between intraseasonal variability and mean state bias in AGCM simulations, *J. Clim.*, *24*(21), 5506–5520.

Kim, D., A. H. Sobel, A. D. Del Genio, Y. Chen, S. J. Camargo, M.-S. Yao, M. Kelley, and L. Nazarenko (2012), The tropical subseasonal variability simulated in the NASA GISS general circulation model, *J. Clim.*, *25*(13), 4641–4659.

Kraucunas, I., and D. L. Hartmann (2005), Equatorial superrotation and the factors controlling the zonal-mean zonal winds in the tropical upper troposphere, *J. Atmos. Sci.*, *62*(2), 371–389, doi:10.1175/JAS-3365.1.

Kumar, S., A. Arora, R. Chattopadhyay, A. Hazra, S. A. Rao, and B. N. Goswami (2016), Seminal role of stratiform clouds in large-scale aggregation of tropical rain in boreal summer monsoon intraseasonal oscillations, *Clim. Dyn.*, pp. 1–17, doi:10.1007/s00382-016-3124-5.

Liebmann, B., and C. Smith (1996), Description of a complete (Interpolated) outgoing longwave radiation dataset., *Bull. Am. Meteorol. Soc.*, *77*, 1275–1277.

Lin, J.-L., G. N. Kiladis, B. E. Mapes, K. M. Weickmann, K. R. Sperber, W. Lin, M. C. Wheeler, S. D. Schubert, A. Del Genio, L. J. Donner, et al. (2006), Tropical intraseasonal variability in 14 IPCC AR4 climate models. Part I: Convective signals, *J. Clim.*, *19*(12), 2665–2690.

Lin, J. W.-B., and J. D. Neelin (2000), Influence of a stochastic moist convective parameterization on tropical climate variability, *Geophys. Res. Lett.*, *27*(22), 3691–3694, doi:10.1029/2000GL011964.

Lin, J. W.-B., and J. D. Neelin (2002), Considerations for stochastic convective parameterization, *J. Atmos. Sci.*, *59*(5), 959–975, doi:10.1175/1520-0469(2002)059<0959:CFSCP>2.0.CO;2.

Lin, J. W.-B., and J. D. Neelin (2003), Toward stochastic deep convective parameterization in general circulation models, *Geophys. Res. Lett.*, *30*(4), doi:10.1029/2002GL016203.

Lin, X., and R. H. Johnson (1996), Heating, moistening, and rainfall over the Western Pacific warm pool during TOGA COARE, *J. Atmos. Sci.*, *53*(22), 3367–3383, doi:10.1175/1520-0469(1996)053<3367:HMAROT>2.0.CO;2.

Majda, A. J., and B. Khouider (2002), Stochastic and mesoscopic models for tropical convection, *Proc. Natl. Acad. Sci. U.S.A.*, *99*(3), 1123–1128, doi:10.1073/pnas.032663199.

Mapes, B., S. Tulich, J. Lin, and P. Zuidema (2006), The mesoscale convection life cycle: Building block or prototype for large-scale tropical waves?, *Dyn. Atmos. Oceans*, *42*(1-4), 3–29, doi:10.1016/j.dynatmoce.2006.03.003.

Mauritsen, T., B. Stevens, E. Roeckner, T. Crueger, M. Esch, M. Giorgetta, H. Haak, J. Jungclaus, D. Klocke, D. Matei, et al. (2012), Tuning the climate of a global model, *J. Adv. Model. Earth Syst.*, *4*(3).

Moncrieff, M. W., D. E. Waliser, M. J. Miller, M. A. Shapiro, G. R. Asrar, and J. Caughey (2012), Multiscale convective organization and the YOTC virtual global field campaign, *Bull. Am. Meteorol. Soc.*, *93*(8), 1171–1187, doi:10.1175/BAMS-D-11-00233.1.

Palmer, T. (1996), On parameterizing scales that are only somewhat smaller than the smallest resolved scales, with application to convection and orography, in *Workshop on New Insights and Approaches to Convective Parametrization, 4-7 November 1996*, pp. 328–337, ECMWF, ECMWF, Shinfield Park, Reading.

Palmer, T. N. (2001), A nonlinear dynamical perspective on model error: A proposal for non-local stochastic-dynamic parametrization in weather and climate prediction models, *Q. J. R. Meteorolog. Soc.*, *127*(572), 279–304, doi:10.1002/qj.49712757202.

Pan, H., and W.-S. Wu (1995), Implementing a mass flux convection parameterization package for the NMC medium-range forecast model, *NMC office note*, *409*(40), 20–233.

Pattanaik, S., S. Abhilash, S. De, A. K. Sahai, R. Phani, and B. N. Goswami (2013), Influence of convective parameterization on the systematic errors of Climate Forecast System (CFS) model over the Indian monsoon region from an extended range forecast perspective, *Clim. Dyn.*, *41*(2), 341–365, doi:10.1007/s00382-013-1662-7.

Peters, K., C. Jakob, L. Davies, B. Khouider, and A. J. Majda (2013), Stochastic behavior of tropical convection in observations and a multicloud model, *J. Atmos. Sci.*, *70*(11), 3556–3575, doi:10.1175/JAS-D-13-031.1.

Peters, K., T. Crueger, C. Jakob, and B. MÃ¶bis (2017), Improved MJO-simulation in ECHAM6.3 by coupling a stochastic multicloud model to the convection scheme, *J. Adv. Model. Earth Syst.*, doi:10.1002/2016MS000809.

Plant, R. S., and G. C. Craig (2008), A stochastic parameterization for deep convection based on equilibrium statistics, *J. Atmos. Sci.*, *65*, 87–105, doi: doi:10.1175/2007JAS2263.1.

Rajeevan, M., J. Bhate, J. Kale, and B. Lal (2006), High resolution daily gridded rainfall data for the indian region: Analysis of break and active, *Current Science*, *91*(3).

Saha, S., S. Moorthi, H.-L. Pan, X. Wu, J. Wang, S. Nadiga, P. Tripp, R. Kistler, J. Woollen, D. Behringer, H. Liu, D. Stokes, R. Grumbine, G. Gayno, J. Wang, Y.-T. Hou, H.-Y. Chuang, H.-M. H. Juang, J. Sela, M. Iredell, R. Treadon, D. Kleist, P. Van Delst, D. Keyser, J. Derber, M. Ek, J. Meng, H. Wei, R. Yang, S. Lord, H. Van Den Dool, A. Kumar, W. Wang, C. Long, M. Chelliah, Y. Xue, B. Huang, J.-K. Schemm, W. Ebisuzaki, R. Lin, P. Xie, M. Chen, S. Zhou, W. Higgins, C.-Z. Zou, Q. Liu, Y. Chen, Y. Han, L. Cucurull, R. W. Reynolds, G. Rutledge, and M. Goldberg (2010), The NCEP Climate Forecast System reanalysis, *Bull. Am. Meteorol. Soc.*, *91*(8), 1015–1057, doi: 10.1175/2010BAMS3001.1.

Saha, S., S. Moorthi, X. Wu, J. Wang, S. Nadiga, P. Tripp, D. Behringer, Y.-T. Hou, H.-y. Chuang, M. Iredell, M. Ek, J. Meng, R. Yang, M. P. Mendez, H. van den Dool, Q. Zhang, W. Wang, M. Chen, and E. Becker (2014), The NCEP Climate Forecast System version 2, *J. Clim.*, *27*(6), 2185–2208, doi:10.1175/JCLI-D-12-00823.1.

Saravanan, R. (1993), Equatorial superrotation and maintenance of the general circulation in two-level models, *J. Atmos. Sci.*, *50*(9), 1211–1227.

Schumacher, C., M. H. Zhang, and P. E. Ciesielski (2007), Heating structures of the TRMM field campaigns, *J. Atmos. Sci.*, *64*(7), 2593–2610, doi:10.1175/JAS3938.1.

Straub, K. H., P. T. Haertel, and G. N. Kiladis (2010), An analysis of convectively coupled kelvin waves in 20 WCRP CMIP3 global coupled climate models, *J. Clim.*, *23*(11), 3031–3056, doi:10.1175/2009JCLI3422.1.

Takayabu, Y. N. (1994), Large-scale cloud disturbances associated with equatorial waves. Part II: Westward-propagating inertio-gravity waves, *J. Meteorol. Soc. Jpn.*, *72*(3), 451–465.

Teixeira, J., and C. A. Reynolds (2008), Stochastic nature of physical parameterizations in ensemble prediction: A stochastic convection approach, *Mon. Weather Rev.*, *136*(2), 483–496, doi:10.1175/2007MWR1870.1.

Waliser, D., K. Jin, I.-S. Kang, W. Stern, S. Schubert, M. Wu, K.-M. Lau, M.-I. Lee, V. Krishnamurthy, A. Kitoh, et al. (2003), AGCM simulations of intraseasonal variability associated with the Asian summer monsoon, *Clim. Dyn.*, *21*(5-6), 423–446.

Wheeler, M., and G. N. Kiladis (1999), Convectively coupled equatorial waves: Analysis of clouds and temperature in the wavenumber-frequency domain, *J. Atmos. Sci.*, *56*(3), 374–399, doi:10.1175/1520-0469(1999)056<0374:CCEWAO>2.0.CO;2.

Yanai, M., S. Esbensen, and J.-H. Chu (1973), Determination of bulk properties of tropical cloud clusters from large-scale heat and moisture budgets, *J. Atmos. Sci.*, *30*(4), 611–627.